



Fatty acid, triglyceride, and kinetic properties of milk fat fractions made by the combination of dry fractionation and short-path molecular distillation

Huiquan Zhu,^{1,2*} Xin Si,^{1,3*} Yunna Wang,¹ Panpan Zhu,^{1,3} Xiaoyang Pang,¹ Xiaodan Wang,¹ Marie-Laure Fauconnier,² Ning Ju,³† Shuwen Zhang,¹† and Jiaping Lv¹‡

¹Institute of Food Science and Technology, Chinese Academy of Agricultural Sciences, Beijing 100193, China

²Laboratory of Chemistry of Natural Molecules, Gembloux Agro-bio Tech, University of Liege, Gembloux 5030, Belgium

³School of Food & Wine, Ningxia University, Yinchuan, Ningxia 750000, China

ABSTRACT

In this study, we aimed to detect the physicochemical properties of distilled products (residue and distillate) obtained from anhydrous milk fat (AMF) and its dry fractionation products (liquid and solid fractions at 25°C [25 L and 25 S]). The results showed that the saturated fatty acids and low- and medium molecular-weight triglycerides were easily accumulated in the distillate, and the percentage of unsaturated fatty acid and high molecular-weight triglycerides in the residue were higher, and these components in 25 S and 25 L were influenced more significantly than those in the AMF. In addition, the distillate had larger melting ranges in comparison with the distilled substrate, while the melting ranges of residue was smaller. The triglycerides were presented as the mixture crystal forms (α , β' , and β crystal) in 25 S, AMF, and their distilling products, and it was transformed gradually to a single form as the increasing of distilling temperature. Moreover, the accumulated pattern of triglycerides was double chain length in 25 S, AMF, and their distilling products. These results provide a new approach to obtain the milk fat fractions with different properties, and the findings of this study enrich the theoretical basis of milk fat separation in practical production.

Key words: dry fractionation, short-path molecular distillation, milk fat, physicochemical property

INTRODUCTION

Milk fat (MF) is an important component of dairy products, accounting for 3 to 5% of total milk, and it is widely used in the baking and catering industry because of its natural smell, good sensory characteristics, and nutritive value (Mohan et al., 2021). Milk fat is com-

posed mainly of triglycerides (TAG, 98%), phospholipids (1–2%), and free fatty acids (<1%; Verma et al., 2020). Moreover, the melting point of MF varies from –30°C to 40°C, which results in certain TAG molecular species being crystallized at a relatively lower temperature than their own melting point. (Boudreau and Arul, 1993). Depending on the melting properties, MF can be classified into high-, medium-, and low-melting fractions, and many researchers have focused recently on how to obtain different MF fractions through various processing techniques, including solvent fractionation, dry fractionation (DF), short-path molecular distillation (SPMD), emulsification fractionation, and so on (Deffense, 1993; Jensen, 2002; Lopez et al., 2006; Anankanbil et al., 2018).

The DF technique is widely used in practical production because of its simple steps and clean products, among other advantages. Dry fractionation involves, first, bringing the MF to a preset temperature, then it is cooled to crystallization and separated successfully into liquid and solid fractions through the solid-liquid separation technique (Bonomi et al., 2012). Studies have reported that, following DF, the short-chain SFA (SC-SFA), UFA, and low molecular-weight TAG (LMW-TAG) have accumulated in the liquid fraction, whereas the percentage of long-chain SFA (LC-SFA) has increased significantly in the solid fraction (Boudreau and Arul, 1993; O'Shea et al., 2000). Wang et al. (2019) found that the percentage of LC-SFA and TAG with 3 SFA in the high-melting point fraction were higher than that in the low-melting point fraction. Moreover, they found that no crystallization had occurred in the low-melting point fraction, while the change from β crystal to β' crystal was observed in the high-melting point fraction and anhydrous MF (AMF; Wang et al., 2019). The same phenomenon was reported by Si et al. (2023) which showed that the high-melting point fractions were mixed mainly with β' crystal at room temperature (Si et al., 2023).

Short-path molecular distillation is an effective liquid-liquid separation technology based on the dif-

Received October 31, 2022.

Accepted April 14, 2023.

*These authors contributed equally to this work.

†Corresponding authors: juming1122@163.com and zswcaas@hotmail.com

ference existing in the molecular average free path of distilling substrate, and its operating temperature is lower compared with other separation methods. Therefore, it is suitable for separating MF or other heat-sensitive bioactive substances, and MF is separated into a light phase (distillate) and a heavy phase (residue) after SPMD (Campos et al., 2003; Berti et al., 2018). Berti et al. (2018) reported that the distillate yield was 30.48%, and the sensory characteristics of distillate were similar to those of AMF (Berti et al., 2018). Other literatures have shown that the percentages of SC-SFA and medium-chain SFA (MC-SFA) in the distillate were higher than those in the residue, while the easier accumulation of LC-SFA and UFA were observed in the residue. Furthermore, the solid fat content decreased in the distillate, and it was reverse variation in the residue (Arul et al., 1988; Campos et al., 2003).

Much of the research on MF separation thus far has focused only on the single separation method, and the development of more efficient separating methods and special MF fractions is, therefore, necessary. In this study, the fatty acids (FA), TAG, thermodynamic properties, and crystal structure of distilled fractions were detected after the combination of DF and SPMD, and these results would provide additional basic information for MF industrialization as well as a new MF separation approach.

MATERIALS AND METHODS

Because no human or animal subjects were used, this analysis did not require approval by an Institutional Animal Care and Use Committee or Institutional Review Board.

Materials

The AMF was purchased from Anchor (Fonterra Co-operative Group Limited, New Zealand). 1,3 (d 5)-diheptadecanoyl-2-heptadecenoyl-glycerol (d 5-(17:0/17:1/17:0) TAG) was selected as the internal standard and was purchased from Avanti Polar Lipids (Birmingham, AL, USA). Methanol, hydrochloric acid (HCL), ethyl alcohol, n-Hexane, acetonitrile, isopropanol, chloroform (CHCl₃), formic acid, and ammonium formate were bought from Fisher Scientific (Pittsburgh, PA, USA). The standard mixture, comprised of 37 FAME, was bought from ANPEL Laboratory Technologies Inc. (Shanghai, China).

MF Separation

As shown in Figure 1, the AMF was heated at 80°C, 70°C, 60°C, 50°C, 40°C, and 30°C in a water bath for

30 min at a time. After heating, the AMF was left to stand in a constant temperature condition (30°C) for 24 h, and then it was separated into solid (30 S) and liquid (30 L) fractions (1,500 rpm, 10 min). The 30 L fraction was subsequently selected to obtain the solid (25 S) and 25 liquid (25 L) fractions at 25°C. For the SPMD process, the AMF, 25 L, and 25 S fractions were distilled at 180°C, 200°C, and 220°C, respectively, with the rate and temperature of the feed port (oil bath) set to 2.0 mL/min and 60°C respectively. The working pressure was 0.1 pa and the speed of the film blade was 150 r/min. When the SPMD temperature was changed, the machine was cleaned with absolute ethyl alcohol. Finally, the AMF was divided into light and heavy phases (distillate and residue), which were collected and stored at 4°C for further analysis.

FA Analysis

The FA were detected using a gas chromatography flame ion detector (GC-FID, Agilent 8890B, Agilent Technologies Inc., CA, USA) equipped with a capillary column (DB-23 60 m × 0.25 mm × 0.25 μm; Sigma-Aldrich, MO, USA; Zhu et al., 2022). Specifically, the MF samples (30 mg) were dissolved in the solution (n-Hexane/methanol/HCL), 2/7/1, vol/vol/v), and the mixture was shocked for 2 min and then heated in a water bath at 100°C for 1 h. The solution was then cooled to room temperature and 2 mL distilled water was added when the heating process was finished. Subsequently, the solution was vortexed (1 min) and centrifuged (1,500 × g, 5 min), and the supernatant liquid was obtained finally for GC analysis. The setting conditions of GC-FID were as follows: the temperatures of the injection port and FID were all 250°C; the carrier gas was high purity nitrogen (99.99999%), and its rate was 0.8 mL/min. For the temperature program, the initial temperature was 50°C, where after it was heated to 175°C at a speed of 20°C/min. Thereafter, the column temperature was increased to 230°C at the rate of 1.3°C/min and stabilized at 230°C for 5 min.

TAG Profile

The TAG detection method was described by previous studies (Wang et al., 2022; Si et al., 2023). First, the samples (5 mg) were dissolved in a solution (methanol/chloroform, 1/2) to a specific concentration (5 mg/mL), and then the sample solution (20 μL), internal standard (5 μL), and methanol (975 μL) were pipetted into a liquid vial for analysis. For the setting condition of the ultra-high liquid chromatography system (I-class Acquity UPLC, Waters Corporation, Milford, USA), the BEH C18 column (1.7 μm, 2.1 mm i.d. ×

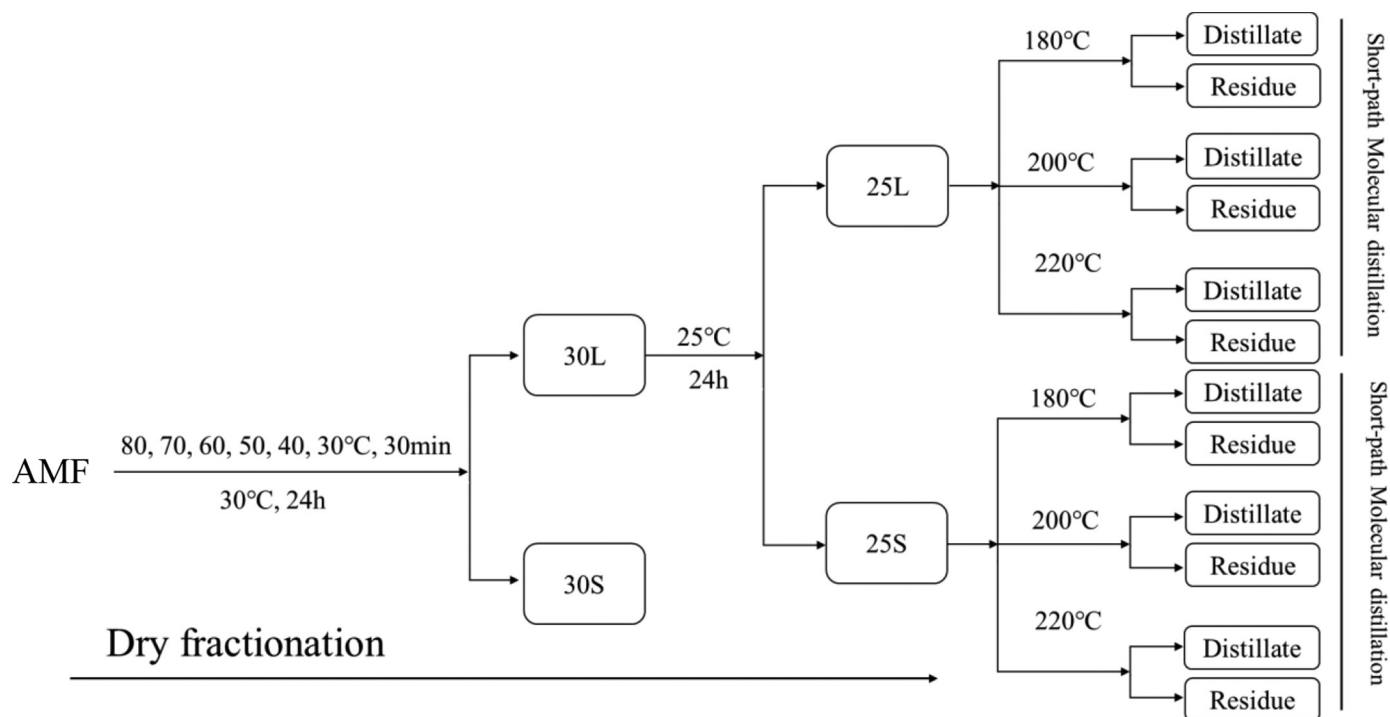


Figure 1. Schematic diagram of the separation process integrated with dry fractionation and short-path molecular distillation. AMF = anhydrous milk fat; 30 L = liquid fraction at 30°C; 30 S = solid fraction at 30°C; 25 L = liquid fraction at 25°C; 25 S = solid fraction at 25°C.

100 mm, Waters Corporation) was chosen to transfer the sample solution. Solvents A (acetonitrile/water, 1/1, vol/vol) and B (isopropanol/acetonitrile, 9:1, vol/vol) both contained 10 mM ammonium formate and 0.1% formic acid; and the flow rate and column temperature was 0.3 mL/min and 60°C respectively. For the MS parameters (API 4500 Q-Trap, AB SCIEX, Framingham, MA, USA), the process started with the acquisition of the parent ion scanning mode; and its bunching potential, mass range, and scanning rate were 100 V, 400–1,200 m/z , and 1,000 Da/s, respectively. The multiple response monitoring (MRM; Q1 = Q3), information dependent acquisition, and enhancement product ion (EPI) were set and used to detect specific FA, and the TAG with different structures were then identified via the MRM. For EPI mode, the inputting range of mass was 50 to 1,200 m/z , and the collision energy was 45 V. The parent ions and characteristic fragment ions were fed into monitoring modes, and the percentage of TAG was calculated by the normalization method of the peak areas.

Thermodynamic Properties and Crystal Form

A differential scanning calorimeter (DSC; DSC 8000, PerkinElmer, Inc., MA, USA) was used to analyze the crystallization and melt process of the sample. The

samples (6–9 mg) were weighed and placed in an empty alumina crucible for detection via the DSC machine. The initial DSC temperature was set to 25°C, and it was then heated to 80°C at the rate of 20°C/min and kept stable for 10 min. In the cooling process, the DSC temperature decreased to –30°C at the rate of 10°C/min, then stabilized for 10 min to obtain the crystallization curve. In the final stage, the temperature increased again to 80°C to acquire the melting curve. The carrier gas was high purity nitrogen (99.9999%) with a flow rate of 20 mL/min. The TAG polymorphism was detected at 25°C for 48 h using the X-ray diffraction (XRD, BTX III, Olympus Corporation, Japan). The power of the optical tube was 2.2 kW, the voltage was 40 kV, and the current was 40 mA; the widths of the emitting slit, antireflection slit, and receiving slit were fixed at 1.0 mm, 1.0 mm, and 0.1 mm, respectively; the scanning rate was 2.0°/min and the 2θ angle ranged from 10.0° to 40.0°.

Statistical Analysis

The results of samples were expressed as mean values \pm standard deviation. One-way ANOVA (ANOVA) was performed to analyze the data, and the significant differences among groups were determined by the Duncan multiple-range tests (SPSS 24.0 software, Chicago, IL,

USA). GraphPad Prism 8 (San Diego, CA, USA) was used for figures processing.

RESULTS AND DISCUSSION

Distillate Yield

Although we detected some efficient ways to separate MF, such as supercritical fluid extraction, SPMD, DF, and other chemical or enzyme extraction methods, the combination of different separation methods has not yet been reported. In this current research, the SPMD was integrated with DF for MF separation, and the AMF, 25 L, and 25 S were distilled at 180°C, 200°C, and 220°C, respectively. The distillate yield MF was obtained using the ratio of the mass of distillate to the mass of total MF. As shown in Figure 2, the distillate yield was positively correlated with the distilling temperature. When the distilling temperature was 180°C, the distillate yield was 6.5% of 25 L, followed by AMF (3.9%) and 25 S (2.4%). The distillate yield of distilling substrates all showed an increasing trend with the increase of temperature, which was in accordance with the previous results (Campos et al., 2003). However, the distillate yield of 25 L was the highest at each distilling temperature, while the distillate yield of AMF and 25 S was in the middle and the lowest, respectively.

FA Variations

FA is the basic component of MF and have a strong correlation with the absorption, metabolism, and processing properties of MF (Małkowska et al., 2021). Based on its saturation, FA can be classified into SFA and UFA; MF is composed mainly of SFA, comprising approximately 2-thirds of its total FA (Gómez-Cortés et al., 2018). In this study, it was evident that the FA proportion of AMF, 25 S, 25 L, and their distilling products was significantly influenced by the DF and SPMD (Tables 1 and 2, graphs A-G in Figures 3 and 4). Specifically, the proportion of SC-SFA and MC-SFA increased comparatively more in 25 L than that in AMF and 25 S ($P < 0.05$), and the LC-SFA remained stable in 25 S and 25 L. For the UFA, the percentage of polyunsaturated FA (PUFA) increased in 25 S and 25 L, while monounsaturated FA (MUFA) showed the reverse variation. However, a previous study demonstrated that the proportion of SFA decreased in all liquid fractions, at both low and high fractionating temperatures (Wang et al., 2019). This contrasting phenomenon might be caused by the difference of DF process among these studies.

For the distilling products, the percentages of SC-SFA and MC-SFA increased at first and then decreased

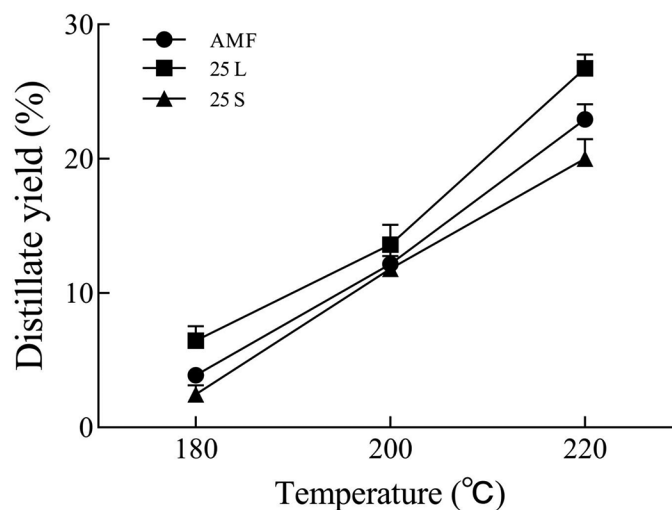


Figure 2. Distillate yield (wt/wt) obtained from AMF, 25 L, and 25 S at various distillation temperatures. The plotted point is the average value, and the error bars represent the standard deviation. AMF = anhydrous milk fat; 25 L = liquid fraction at 25°C; 25 S = solid fraction at 25°C.

in the distillate of all distilling substrates. However, these FA saw a decrease in residue ($P < 0.05$), concurring with the phenomenon reported by Arul et al. (1988). For the LC-SFA, the percentage of myristic acid (C14:0) showed the same variation with SC-SFA and MC-SFA, and the proportions of pentadecanoic acid (C15:0) and palmitic acid (C16:0) remained stable, while the stearic acid (C18:0) was different in that its percentage decreased and rose in the distillate and residue, respectively. However, the UFA demonstrated opposite variations compared with SFA. The percentages of oleic acid (C18:1n9c), linoleic acid (C18:2n6c), trans linoleic acid (C18:2n6t), and linolenic acid (C18:3n6) all decreased in the distillate, but showed an increasing trend in the residue, which was concurred with results reported by previous literature (Campos et al., 2003). It was worth mentioning that the FA percentages in 25 S and 25 L were affected obviously by the SPMD compared with that in AMF, which might be caused by the different melting points of FA, such as 54.4°C for C14:0, 62.9°C for C16:0, and 69.6°C for C18:0 (Lopez et al., 2006; Tzompa-Sosa et al., 2014).

TAG Variations

The physical and chemical properties of TAG directly determine the quality and characteristic of milk products, such as cream and butter (Silva et al., 2014). In the current study, a total of 44 TAG molecular species were detected (Tables 3 and 4). These TAG molecular species were classified into 3 groups based on the length

Table 1. Fatty acids in distillate of each fraction¹

Fatty acid	AMF						25 L						25 S								
	Room temperature (°C)		Distilling temperature (°C)		Room temperature (°C)		Distilling temperature (°C)		Room temperature (°C)		Distilling temperature (°C)		Room temperature (°C)		Distilling temperature (°C)						
	180	200	180	200	180	200	180	200	180	200	180	200	180	200	180	200					
C4:0	1.05 ± 0.05 ^a	1.63 ± 0.24 ^b	1.50 ± 0.02 ^b	1.77 ± 0.01 ^b	1.49 ± 0.01 ^a	2.13 ± 0.00 ^b	2.40 ± 0.04 ^c	2.19 ± 0.02 ^b	1.15 ± 0.12 ^a	1.82 ± 0.01 ^b	1.83 ± 0.08 ^b	1.69 ± 0.01 ^b	1.70 ± 0.03 ^a	2.17 ± 0.12 ^b	2.10 ± 0.03 ^b	2.23 ± 0.00 ^b	2.34 ± 0.02 ^b	1.60 ± 0.09 ^a	2.34 ± 0.02 ^b	2.20 ± 0.04 ^b	2.17 ± 0.01 ^b
C6:0	1.52 ± 0.05 ^a	1.91 ± 0.06 ^b	1.97 ± 0.03 ^b	1.94 ± 0.02 ^b	2.05 ± 0.02 ^a	2.7 ± 0.04 ^{bc}	2.75 ± 0.04 ^c	2.62 ± 0.02 ^b	1.68 ± 0.02 ^a	2.67 ± 0.05 ^b	2.43 ± 0.02 ^c	2.17 ± 0.02 ^d	1.86 ± 0.01 ^d	3.43 ± 0.12 ^a	4.35 ± 0.05 ^b	4.30 ± 0.02 ^b	4.62 ± 0.03 ^d	1.44 ± 0.07 ^a	2.49 ± 0.04 ^b	2.19 ± 0.04 ^c	1.86 ± 0.01 ^d
C8:0	6.54 ± 0.16 ^a	8.43 ± 0.04	8.43 ± 0.04	8.72 ± 0.02 ^b	7.14 ± 0.01 ^a	9.88 ± 0.13 ^b	10.10 ± 0.05 ^b	9.03 ± 0.05 ^c	3.77 ± 0.00 ^a	5.63 ± 0.08 ^b	5.27 ± 0.03 ^c	4.62 ± 0.03 ^d	4.15 ± 0.02 ^d	13.75 ± 0.97 ^a	14.32 ± 0.20 ^a	14.61 ± 2.01 ^a	16.47 ± 0.08 ^d	3.46 ± 0.08 ^a	5.52 ± 0.11 ^c	5.02 ± 0.12 ^c	4.15 ± 0.02 ^d
C10:0	1.48 ± 0.05 ^a	2.26 ± 0.03 ^b	2.24 ± 0.02 ^b	2.50 ± 0.09 ^c	1.78 ± 0.01 ^a	2.37 ± 0.01 ^a	2.12 ± 0.35 ^a	1.68 ± 0.04 ^a	7.19 ± 0.07 ^a	15.69 ± 0.05 ^b	17.08 ± 0.10 ^b	16.47 ± 0.08 ^d	15.91 ± 0.02 ^b	13.75 ± 0.97 ^a	14.32 ± 0.20 ^a	14.61 ± 2.01 ^a	16.47 ± 0.08 ^d	14.4 ± 0.01 ^a	16.41 ± 0.16 ^{bc}	17.00 ± 0.30 ^c	15.91 ± 0.02 ^b
C12:0	1.15 ± 0.06 ^a	1.27 ± 0.03 ^{ab}	1.27 ± 0.03 ^{ab}	1.39 ± 0.06 ^b	1.20 ± 0.03 ^a	1.29 ± 0.01 ^b	1.42 ± 0.01 ^c	1.40 ± 0.02 ^c	1.57 ± 0.01 ^a	1.26 ± 0.05 ^a	1.29 ± 0.01 ^{ab}	1.40 ± 0.02 ^c	1.38 ± 0.00 ^b	1.72 ± 0.08 ^a	3.07 ± 0.05 ^b	2.94 ± 0.01 ^b	2.89 ± 0.09 ^b	1.26 ± 0.05 ^a	1.29 ± 0.01 ^{ab}	1.40 ± 0.02 ^b	1.38 ± 0.00 ^b
C14:0	33.35 ± 1.06 ^a	30.76 ± 0.26 ^a	31.87 ± 1.00 ^a	31.89 ± 0.03 ^a	31.16 ± 0.00 ^a	29.29 ± 0.03 ^b	31.37 ± 0.19 ^a	32.98 ± 0.02 ^c	33.15 ± 0.14 ^a	30.76 ± 0.26 ^a	30.48 ± 0.06 ^b	32.16 ± 0.05 ^c	33.69 ± 0.28 ^a	1.72 ± 0.08 ^a	3.07 ± 0.05 ^b	2.94 ± 0.01 ^b	2.89 ± 0.09 ^b	33.15 ± 0.14 ^a	30.48 ± 0.06 ^b	32.16 ± 0.05 ^c	33.69 ± 0.28 ^a
C16:1	0.54 ± 0.06 ^a	0.35 ± 0.03 ^b	0.35 ± 0.03 ^b	0.33 ± 0.01 ^b	0.40 ± 0.02 ^a	0.33 ± 0.01 ^a	0.33 ± 0.03 ^a	0.34 ± 0.03 ^a	0.40 ± 0.03 ^a	0.33 ± 0.01 ^a	0.33 ± 0.01 ^a	0.33 ± 0.03 ^a	0.31 ± 0.00 ^b	0.21 ± 0.03 ^a	0.19 ± 0.02 ^a	0.20 ± 0.02 ^a	0.22 ± 0.01 ^a	0.40 ± 0.03 ^a	0.33 ± 0.03 ^a	0.33 ± 0.03 ^a	0.31 ± 0.00 ^b
C17:1	8.50 ± 0.50 ^a	8.61 ± 0.13 ^a	8.17 ± 1.55 ^a	8.09 ± 0.20 ^a	8.99 ± 0.46 ^a	6.36 ± 0.15 ^b	5.70 ± 0.42 ^b	7.08 ± 0.45 ^b	8.25 ± 0.21 ^a	6.36 ± 0.15 ^b	5.70 ± 0.42 ^b	7.08 ± 0.45 ^b	6.80 ± 0.25 ^a	21.74 ± 0.64 ^a	17.81 ± 0.30 ^b	16.75 ± 2.18 ^b	15.24 ± 0.02 ^b	8.25 ± 0.21 ^a	7.12 ± 0.30 ^a	6.76 ± 0.73 ^a	6.80 ± 0.25 ^a
C18:0	0.31 ± 0.03 ^a	0.47 ± 0.02 ^a	0.42 ± 0.16 ^a	0.37 ± 0.02 ^a	0.80 ± 0.00 ^a	0.66 ± 0.13 ^a	0.62 ± 0.10 ^a	0.66 ± 0.05 ^a	1.18 ± 0.03 ^a	0.66 ± 0.13 ^a	0.62 ± 0.10 ^a	0.66 ± 0.05 ^a	0.81 ± 0.23 ^a	2.07 ± 0.14 ^a	2.05 ± 0.03 ^a	1.95 ± 0.57 ^a	1.98 ± 0.02 ^a	1.18 ± 0.03 ^a	0.32 ± 0.01 ^b	0.82 ± 0.04 ^a	0.81 ± 0.23 ^a
C18:1n9c	0.66 ± 0.04 ^a	0.51 ± 0.00 ^{ab}	0.52 ± 0.00 ^b	0.54 ± 0.02 ^{ab}	0.68 ± 0.02 ^a	0.58 ± 0.01 ^b	0.51 ± 0.00 ^c	0.52 ± 0.00 ^c	0.55 ± 0.02 ^a	0.58 ± 0.01 ^b	0.51 ± 0.00 ^c	0.52 ± 0.00 ^c	0.49 ± 0.01 ^a	0.66 ± 0.04 ^a	0.51 ± 0.00 ^{ab}	0.52 ± 0.00 ^b	0.54 ± 0.02 ^{ab}	0.55 ± 0.02 ^a	0.54 ± 0.04 ^a	0.50 ± 0.01 ^a	0.49 ± 0.01 ^a

^{a-d}Different letters within the same row are significantly different ($P < 0.05$).

¹AMF: anhydrous milk fat; 25 L: liquid fraction at 25°C; 25 S: solid fraction at 25°C.

Table 2. Fatty acids in residue of each fraction¹

Fatty acid	AMF											
	25 L						25 S					
	Room temperature (°C)		Distilling temperature (°C)		Room temperature (°C)		Distilling temperature (°C)		Room temperature (°C)		Distilling temperature (°C)	
180	200	180	200	180	200	180	200	180	200	180	200	
C4:0	1.05 ± 0.05 ^a	1.12 ± 0.04 ^a	0.79 ± 0.00 ^b	0.90 ± 0.02 ^b	1.49 ± 0.01 ^a	1.42 ± 0.02 ^a	1.10 ± 0.03 ^b	0.96 ± 0.12 ^b	1.15 ± 0.12 ^a	0.99 ± 0.08 ^{ab}	0.80 ± 0.01 ^b	0.50 ± 0.00 ^c
C6:0	1.70 ± 0.02 ^a	1.49 ± 0.05 ^b	1.32 ± 0.02 ^c	1.43 ± 0.02 ^b	2.05 ± 0.02 ^a	1.99 ± 0.01 ^a	1.54 ± 0.05 ^b	1.54 ± 0.19 ^b	1.60 ± 0.09 ^a	1.40 ± 0.1 ^{ab}	1.25 ± 0.04 ^b	0.93 ± 0.00 ^c
C8:0	1.52 ± 0.05 ^a	1.25 ± 0.01 ^b	1.08 ± 0.02 ^c	1.15 ± 0.02 ^c	1.68 ± 0.02 ^a	1.53 ± 0.01 ^b	1.28 ± 0.02 ^c	1.27 ± 0.06 ^c	1.44 ± 0.07 ^a	1.14 ± 0.08 ^b	1.08 ± 0.02 ^b	0.86 ± 0.00 ^c
C10:0	3.43 ± 0.12 ^a	3.12 ± 0.01 ^b	2.70 ± 0.04 ^c	2.83 ± 0.04 ^c	3.77 ± 0.00 ^a	3.42 ± 0.01 ^b	3.10 ± 0.01 ^c	2.99 ± 0.00 ^d	3.46 ± 0.08 ^a	2.90 ± 0.05 ^b	2.60 ± 0.04 ^c	2.44 ± 0.02 ^c
C12:0	6.54 ± 0.16 ^a	6.85 ± 0.02 ^a	5.73 ± 0.05 ^b	5.97 ± 0.07 ^b	7.14 ± 0.01 ^a	6.60 ± 0.00 ^b	5.93 ± 0.05 ^c	5.55 ± 0.01 ^d	7.19 ± 0.07 ^a	6.23 ± 0.12 ^b	5.68 ± 0.03 ^c	5.37 ± 0.06 ^d
C14:0	13.75 ± 0.97 ^a	14.04 ± 0.06 ^a	12.42 ± 0.17 ^a	12.52 ± 0.24 ^a	13.69 ± 0.02 ^a	13.26 ± 0.01 ^a	12.44 ± 0.19 ^b	11.56 ± 0.16 ^c	14.40 ± 0.01 ^a	13.5 ± 0.25 ^b	12.43 ± 0.31 ^c	12.27 ± 0.17 ^c
C14:1	1.48 ± 0.05 ^a	2.38 ± 0.01 ^b	2.27 ± 0.01 ^b	2.23 ± 0.08 ^b	1.78 ± 0.01 ^a	2.47 ± 0.01 ^a	2.37 ± 0.05 ^a	2.26 ± 0.36 ^a	1.57 ± 0.01 ^a	1.46 ± 0.07 ^a	1.43 ± 0.02 ^a	1.47 ± 0.02 ^a
C15:0	1.15 ± 0.06 ^a	1.27 ± 0.00 ^a	1.16 ± 0.02 ^a	1.15 ± 0.04 ^a	1.20 ± 0.03 ^a	1.22 ± 0.00 ^a	1.14 ± 0.03 ^a	1.08 ± 0.06 ^a	1.26 ± 0.05 ^a	1.22 ± 0.03 ^a	1.16 ± 0.03 ^a	1.16 ± 0.02 ^a
C16:0	33.35 ± 1.06 ^a	33.27 ± 0.14 ^a	32.7 ± 0.16 ^a	32.09 ± 0.33 ^a	31.16 ± 0 ^{ab}	31.58 ± 0.05 ^b	31.44 ± 0.32 ^b	30.43 ± 0.31 ^a	33.15 ± 0.14 ^a	33.71 ± 0.04 ^a	33.56 ± 0.42 ^a	32.84 ± 0.26 ^a
C16:1	1.72 ± 0.08 ^a	2.36 ± 0.33 ^b	3.30 ± 0.06 ^c	3.27 ± 0.00 ^f	2.20 ± 0.06 ^a	2.21 ± 0.01 ^a	2.37 ± 0.06 ^a	2.37 ± 0.02 ^a	3.23 ± 0.06 ^a	1.86 ± 0.03 ^b	2.81 ± 0.03 ^c	2.93 ± 0.01 ^c
C17:0	0.54 ± 0.06 ^a	0.35 ± 0.03 ^b	0.46 ± 0.01 ^{ab}	0.33 ± 0.07 ^b	0.40 ± 0.02 ^a	0.39 ± 0.05 ^a	0.52 ± 0.07 ^a	0.44 ± 0.04 ^a	0.40 ± 0.03 ^{ab}	0.34 ± 0.01 ^a	0.37 ± 0.02 ^{ab}	0.41 ± 0.00 ^b
C17:1	0.21 ± 0.03 ^{ab}	0.18 ± 0.01 ^a	0.17 ± 0.01 ^a	0.26 ± 0.01 ^b	0.26 ± 0.00 ^a	0.26 ± 0.02 ^a	0.42 ± 0.06 ^b	0.36 ± 0.02 ^{ab}	0.19 ± 0.01 ^a	0.24 ± 0.03 ^a	0.18 ± 0.01 ^a	0.20 ± 0.00 ^a
C18:0	8.50 ± 0.50 ^a	9.31 ± 0.01 ^{ab}	10.46 ± 0.54 ^{ab}	10.78 ± 0.93 ^b	8.99 ± 0.46 ^a	8.30 ± 0.09 ^a	8.58 ± 0.33 ^a	9.44 ± 0.71 ^a	8.25 ± 0.21 ^a	10.05 ± 0.64 ^b	10.04 ± 0.15 ^b	11.06 ± 0.24 ^b
C18:1n9c	21.74 ± 0.63 ^a	19.72 ± 0.16 ^b	21.79 ± 0.11 ^a	21.27 ± 0.40 ^a	20.48 ± 0.37 ^a	21.82 ± 0.09 ^a	24.51 ± 0.39 ^b	25.76 ± 0.27 ^b	18.96 ± 0.15 ^a	19.63 ± 0.24 ^b	20.91 ± 0.13 ^c	22.74 ± 0.03 ^d
C18:2n6t	0.31 ± 0.03 ^a	0.53 ± 0.02 ^b	0.52 ± 0.00 ^b	0.50 ± 0.04 ^b	0.80 ± 0.00 ^a	0.88 ± 0.07 ^b	1.14 ± 0.10 ^c	0.84 ± 0.02 ^d	1.18 ± 0.03 ^a	1.28 ± 0.04 ^{ab}	1.43 ± 0.03 ^b	1.31 ± 0.07 ^{ab}
C18:2n6c	2.07 ± 0.14 ^a	2.14 ± 0.06 ^a	2.42 ± 0.15 ^a	2.63 ± 0.41 ^a	2.23 ± 0.03 ^a	1.95 ± 0.03 ^a	1.94 ± 0.10 ^a	2.25 ± 0.13 ^a	1.74 ± 0.10 ^a	3.16 ± 0.33 ^b	2.91 ± 0.02 ^b	2.39 ± 0.22 ^{ab}
C18:3n6	0.66 ± 0.04 ^a	0.63 ± 0.03 ^a	0.71 ± 0.05 ^a	0.69 ± 0.03 ^a	0.68 ± 0.02 ^a	0.69 ± 0.05 ^a	0.70 ± 0.02 ^a	0.91 ± 0.07 ^b	0.55 ± 0.02 ^a	0.64 ± 0.00 ^b	0.63 ± 0.00 ^b	0.68 ± 0.01 ^c

^{a-d}Different letters within the same row are significantly different ($P < 0.05$).

¹AMF: anhydrous milk fat; 25 L: liquid fraction at 25°C; 25 S: solid fraction at 25°C.

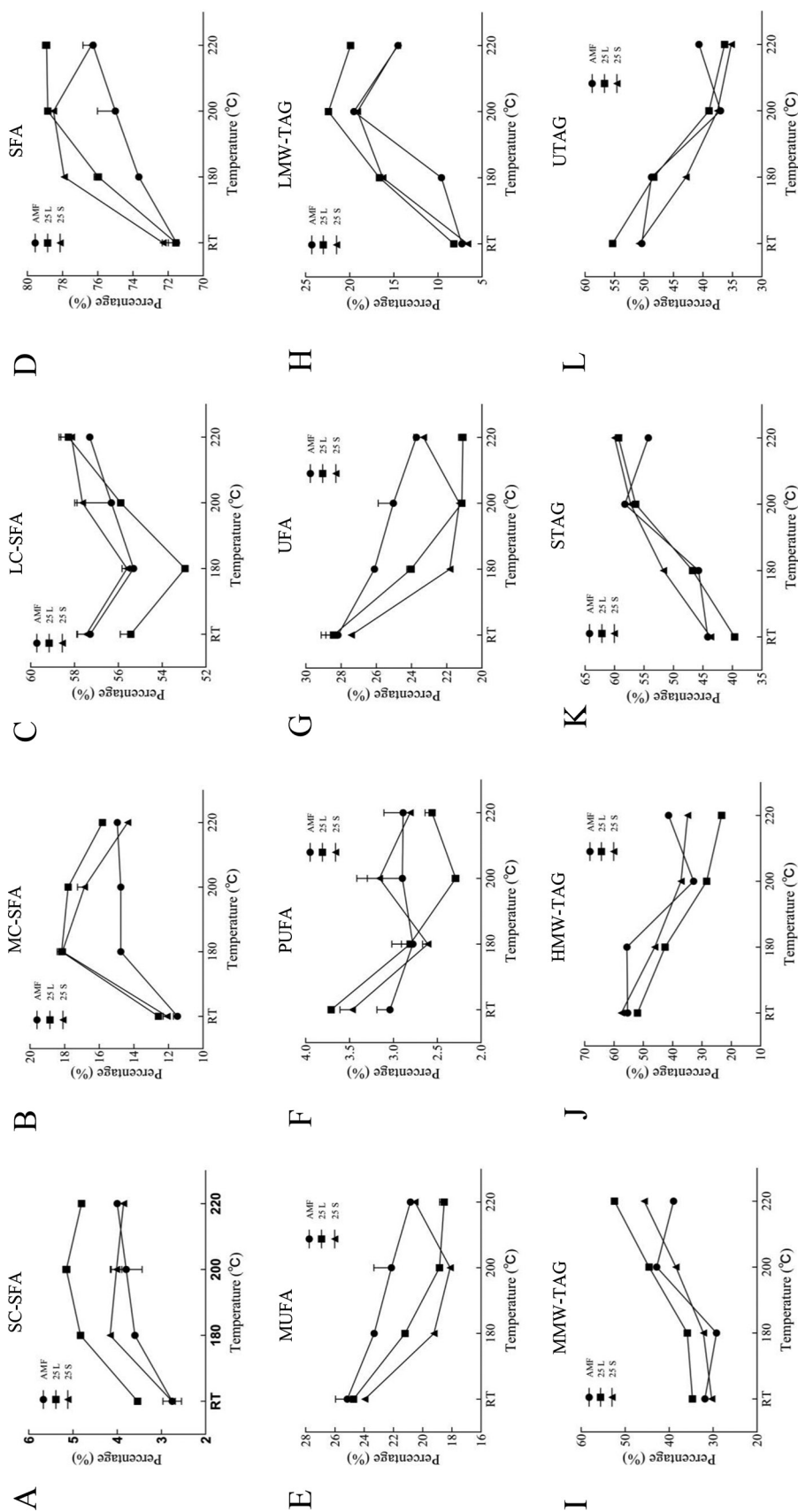


Figure 3. Chemical composition of distillate in AMF, 25 L, and 25 S at different distilling temperatures. The plotted point is the average value, and the error bars represent the standard deviation. SFA = $\Sigma(C4:0, C6:0, C8:0, C10:0, C11:0, C12:0, C14:0, C15:0, C16:0, C17:0, C18:0)$; SC-SFA (short-chain SFA) = $\Sigma(C4:0, C6:0)$; MC-SFA (medium-chain SFA) = $\Sigma(C8:0, C10:0, C11:0, C12:0, C14:0)$; LC-SFA (long-chain SFA) = $\Sigma(C15:0, C16:0, C17:0, C18:0)$; MUFA = $\Sigma(C14:1, C15:1, C16:1, C17:1, C18:1n9c)$; PUFA = $\Sigma(C18:2n6c, C18:3n6)$; UFA = $\Sigma(\text{MUFA and PUFA})$; LMW-TAG (low molecular-weight triglyceride) = $\Sigma(\text{carbon number from 26 to 34})$; MMW-TAG (medium molecular-weight triglyceride) = $\Sigma(\text{carbon number from 35 to 40})$; HMW-TAG (high molecular-weight triglyceride) = $\Sigma(\text{carbon number from 41 to 54})$; STAG = triglyceride with 3 SFA; UTAG = triglyceride with at least 1 UFA; AMF = anhydrous milk fat; 25 L = liquid fraction at 25°C; 25 S = solid fraction at 25°C.

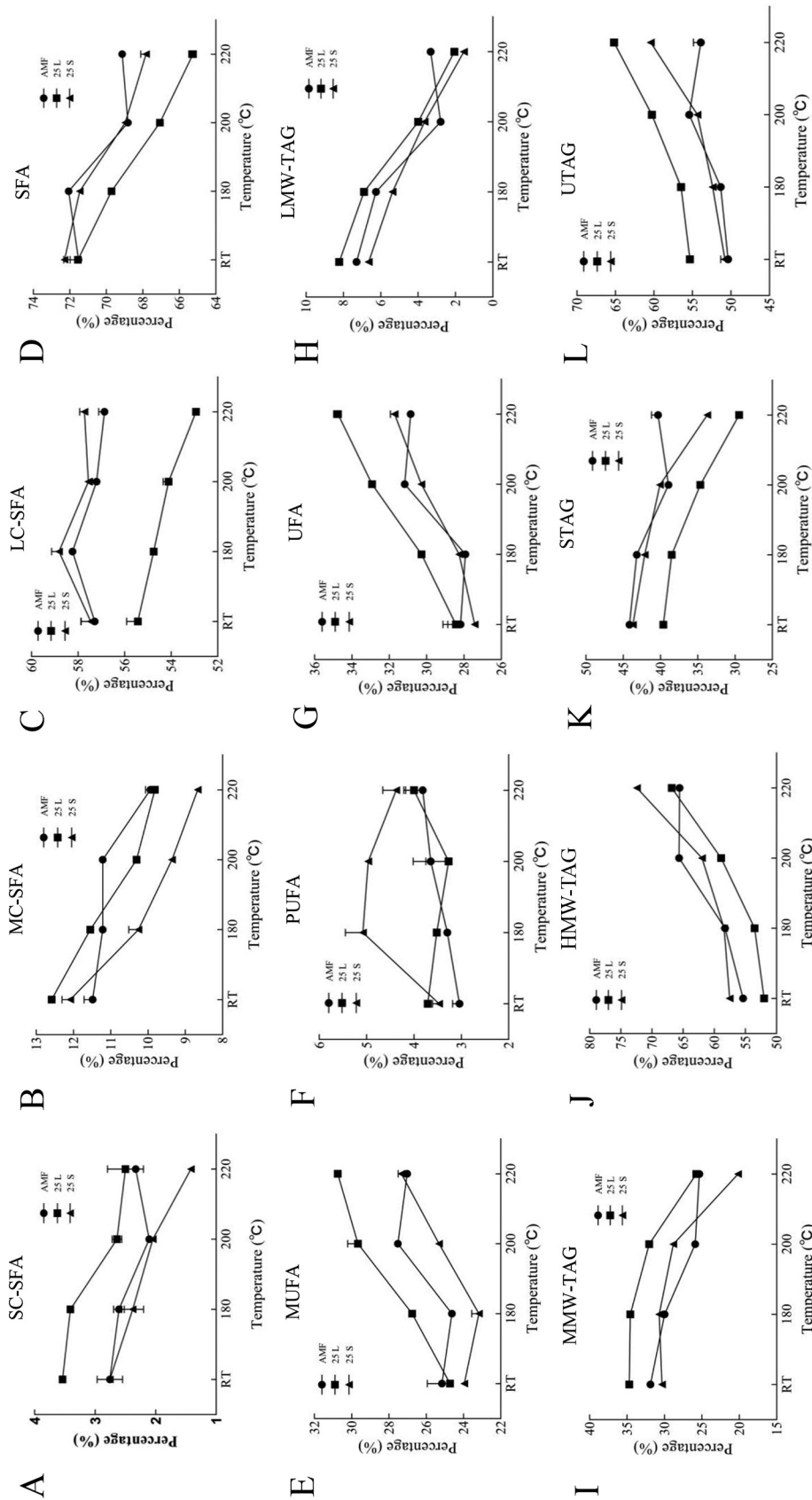


Figure 4. Chemical composition of residue in AMF, 25 L, and 25 S at different distilling temperatures. The plotted point is the average value, and the error bars represent the standard deviation. SFA = $\Sigma(C4:0, C6:0, C8:0, C10:0, C11:0, C12:0, C14:0, C15:0, C16:0, C17:0, C18:0)$; SC-SFA (short-chain SFA) = $\Sigma(C4:0, C6:0)$; MC-SFA (medium-chain SFA) = $\Sigma(C8:0, C10:0, C11:0, C12:0, C14:0)$; LC-SFA (long-chain SFA) = $\Sigma(C15:0, C16:0, C17:0, C18:0)$; MUFA = $\Sigma(C14:1, C15:1, C16:1, C17:1, C18:1n9c)$; PUFA = $\Sigma(C18:2n6c, C18:2n6t, C18:3n6)$; UFA = $\Sigma(\text{MUFA and PUFA})$; LMW-TAG (low molecular-weight triglyceride) = $\Sigma(\text{carbon number from 26 to 34})$; MMW-TAG (medium molecular-weight triglyceride) = $\Sigma(\text{carbon number from 35 to 40})$; HMW-TAG (high molecular-weight triglyceride) = $\Sigma(\text{carbon number from 41 to 54})$; STAG = triglyceride with 3 SFA; UTAG = triglyceride with at least 1 UFA; AMF = anhydrous milk fat; 25 L = liquid fraction at 25°C; 25 S = solid fraction at 25°C.

of acyl-carbon, including LMW-TAG (carbon number: 24–34), medium molecular-weight TAG (MMW-TAG, carbon number: 35–40), and high molecular-weight TAG (HMW-TAG, carbon number: 41–54; Graphs H–J in Figures 3 and 4; Smiddy et al., 2012). The proportions of LMW- and MMW-TAG in the 25 L all were higher than those in the AMF and 25 S. By contrast, the HMW-TAG was accumulated easily in the 25 S, in accordance with the previous results (Boudreau and Arul, 1993; Lopez et al., 2006). During the distilling process, the percentages of LMW- and MMW-TAG increased sharply in all distillates (AMF, 25 L, and 25 S) at 180°C and 200°C, however, these TAG demonstrated a decreasing trend in the residue. These phenomena were also reported by previous studies (Arul et al., 1988; Campos et al., 2003). With the increase of distilling temperature, the proportion of LMW-TAG declined in the all distillates at 220°C. The proportion of MMW-TAG decreased in the AMF distillate at 220°C, but increased continually in the distillate of 25 L and 25 S, the opposite trend was observed in the residue. For HMW-TAG, which accounted for 55.38% of total AMF, it showed the decreasing trend in the distillate. On the contrary, the proportion of HMW-TAG increased in the residue. Another noteworthy finding was that the percentage of LMW-TAG was affected obviously by the SPMD in comparison with MMW- and HMG-TAG.

The TAG can also be classified into saturated TAG (STAG), which contains 3 SFA, and unsaturated TAG (UTAG), which contains at least one UFA. Here, the percentage of STAG increased gradually in the distillate throughout the distilling process (Tables 3 and 4, graphs K–L in Figures 3 and 4). By contrast, the STAG showed a decrease in the residue, and the opposite variation was observed for UTAG. This phenomenon was more evident in the individual TAG molecular species. For instance, the proportion of C52:2 and C52:3 increased from 5.73% and 0.96% to 6.65% and 1.10%, respectively, in the AMF residue, with the increasing rates of 16.10% and 14.58%, respectively. The increasing proportion of C52:2 in residue was 29.71% and 49.45% in 25 L and 25 S, respectively, and those of C52:3 were 32.11% in the 25 L and 36.84% in the 25 S, which all were more apparent in comparison with the AMF. It was reported that C52:2 and C52:3 were mainly composed of C18:1/C16:0/C18:1 and C18:1/C16:0/C18:2, respectively, and they were the major component in the human milk, accounting for 20–40% of total TAG (Zhao et al., 2018; Zhu et al., 2021).

Thermal Characteristics

More than 3 endothermic peaks were observed in the AMF, 25 S, and 25 L (Graphs A, C, and E in Figure

5), which might be caused by the presence of some TAG with different molecular weight, such as LMM-, MMM-, and HMM-TAG in these samples (Fatouh et al., 2003). The melting temperature of AMF ranged from -12.47°C to 37.86°C , a wider range than both 25 S (-0.18°C – 41.19°C) and 25 L (-11.87°C – 25.31°C). Moreover, the first endothermic peak of AMF appeared at -11°C , followed by 25 L (-8°C) and 25 S (9°C), and these results were due to the greater accumulation of LMM- and HMM-TAG in the 25 L and 25 S, respectively (Lohman and Hartel, 1994; Ransom-Painter et al., 1997). The melting temperature range of the distillate was shorter than that of their distilling substrates, however, the residue had a wider melting temperature range. In addition, the appearing temperature of endothermic peak in the distilling products was delayed with the increase of distilling temperature. For example, we detected only one endothermic peak in the distillate of 25 L at 180°C and 200°C. The probable reason for this phenomenon was that there were more LMW-TAG in the distillate of 25 L at the relative low distilling temperature. Moreover, the number of endothermic peaks increased and the appearing position of endothermic peaks shifted to the high-temperature area. The appearing positions for the main endothermic peak of 25 S and its distillate and residue were 37°C , 15°C , and 40°C , respectively. These results indicated that the content of LMW-TAG in the 25 S distillate was higher, while more HMW-TAG accumulated in the 25 S residue, which were correspond with the data shown in Tables 3 and 4.

For the crystallization curves, 25 S first crystallized at 18.23°C , followed by AMF (12.60°C) and 25 L (8.90°C ; Graphs B, D, and F in Figure 5). We detected 3 exothermic peaks in 25 S compared with 2 in AMF and one in 25 L, probably because 25 S had a higher proportion of HMW-TAG (Lopez et al., 2001). Moreover, the appearing position of exothermic peaks in all distilling products moved gradually to the high-temperature region as the distilling temperature increased, and the crystallization temperature of residue was higher than that of distillate at the same distilling temperature. Three exothermic peaks were constantly observed in the residues of 25 S and AMF, but the number of exothermic peaks decreased gradually to one in their distillates. In addition, only one exothermic peak was observed in the residues and distillates of 25 L, which might be caused by the percentage of HMW-TAG in 25 L and its distilling products was relatively low (Lopez et al., 2001; Wang et al., 2019). The detailed correlation between the peak points of exothermic peak and crystal forms in crystallization curve had been previously reported, including low-, medium-, and high-temperature exothermic peaks (0 – 10°C , 20 – 40°C ,

Table 3. Triglyceride in distillate of each fraction¹

Triglyceride	AMF						25 L						25 S					
	Room temperature (°C)		Distilling temperature (°C)		Room temperature (°C)		Distilling temperature (°C)		Room temperature (°C)		Distilling temperature (°C)		Room temperature (°C)		Distilling temperature (°C)			
	180	200	180	200	180	200	180	200	180	200	180	200	180	200	180	200		
26:0	0.02 ± 0.00 ^a	0.07 ± 0.00 ^b	0.08 ± 0.00 ^b	0.06 ± 0.00 ^b	0.02 ± 0.00 ^a	0.1 ± 0.01 ^c	0.16 ± 0.00 ^b	0.1 ± 0.01 ^c	0.08 ± 0.00 ^d	0.02 ± 0.00 ^a	0.15 ± 0.00 ^b	0.11 ± 0.00 ^c	0.15 ± 0.00 ^b	0.06 ± 0.00 ^d				
28:0	0.06 ± 0.00 ^a	0.21 ± 0.01 ^b	0.19 ± 0.01 ^b	0.18 ± 0.01 ^b	0.07 ± 0.00 ^a	0.28 ± 0.02 ^b	0.36 ± 0.01 ^b	0.28 ± 0.02 ^b	0.21 ± 0.01 ^d	0.05 ± 0.00 ^a	0.34 ± 0.01 ^b	0.29 ± 0.00 ^b	0.34 ± 0.01 ^b	0.15 ± 0.00 ^c				
30:0	0.65 ± 0.01 ^a	1.42 ± 0.02 ^a	1.42 ± 0.02 ^a	1.79 ± 0.01 ^d	0.75 ± 0.00 ^a	3.07 ± 0.00 ^b	2.88 ± 0.02 ^b	3.07 ± 0.00 ^b	2.31 ± 0.13 ^c	0.61 ± 0.00 ^a	2.91 ± 0.06 ^b	2.86 ± 0.03 ^b	2.91 ± 0.06 ^b	1.57 ± 0.00 ^c				
32:0	1.16 ± 0.01 ^a	1.72 ± 0.00 ^b	1.72 ± 0.00 ^b	2.60 ± 0.01 ^d	1.33 ± 0.02 ^a	4.40 ± 0.09 ^c	3.25 ± 0.02 ^b	4.40 ± 0.09 ^c	3.53 ± 0.05 ^d	1.08 ± 0.00 ^a	3.25 ± 0.04 ^b	3.74 ± 0.05 ^c	3.25 ± 0.04 ^b	2.59 ± 0.02 ^d				
34:0	4.26 ± 0.08 ^a	4.84 ± 0.15 ^b	4.84 ± 0.15 ^b	10.51 ± 0.21 ^c	4.77 ± 0.06 ^a	11.17 ± 0.06 ^c	7.76 ± 0.04 ^b	11.17 ± 0.06 ^c	10.57 ± 0.47 ^d	3.84 ± 0.02 ^a	7.39 ± 0.08 ^b	9.24 ± 0.12 ^c	7.39 ± 0.08 ^b	7.90 ± 0.06 ^d				
34:1	1.15 ± 0.00 ^a	1.36 ± 0.01 ^b	1.36 ± 0.01 ^b	2.84 ± 0.04 ^c	1.29 ± 0.02 ^a	3.41 ± 0.03 ^c	2.23 ± 0.03 ^b	3.41 ± 0.03 ^c	3.22 ± 0.11 ^c	1.04 ± 0.01 ^a	2.25 ± 0.01 ^b	2.90 ± 0.00 ^c	2.25 ± 0.01 ^b	2.34 ± 0.02 ^b				
35:0	0.20 ± 0.00 ^a	0.20 ± 0.00 ^a	0.20 ± 0.00 ^a	0.36 ± 0.01 ^b	0.22 ± 0.00 ^a	0.44 ± 0.01 ^c	0.30 ± 0.00 ^b	0.44 ± 0.01 ^c	0.48 ± 0.02 ^c	0.16 ± 0.00 ^a	0.38 ± 0.01 ^b	0.38 ± 0.01 ^b	0.38 ± 0.01 ^b	0.35 ± 0.01 ^c				
36:0	9.16 ± 0.01 ^a	8.87 ± 0.14 ^b	8.87 ± 0.14 ^b	16.29 ± 0.11 ^c	10.22 ± 0.05 ^a	17.49 ± 0.07 ^c	12.08 ± 0.09 ^b	17.49 ± 0.07 ^c	18.77 ± 0.5 ^d	8.38 ± 0.09 ^a	11.10 ± 0.10 ^b	14.44 ± 0.08 ^c	11.10 ± 0.10 ^b	15.46 ± 0.02 ^d				
36:1	1.14 ± 0.01 ^a	1.19 ± 0.00 ^a	1.19 ± 0.00 ^a	2.3 ± 0.06 ^b	1.37 ± 0.07 ^a	2.38 ± 0.05 ^c	1.77 ± 0.03 ^b	2.38 ± 0.05 ^c	2.66 ± 0.00 ^d	1.1 ± 0.02 ^a	1.54 ± 0.05 ^b	1.95 ± 0.03 ^c	1.54 ± 0.05 ^b	2.09 ± 0.00 ^c				
36:2	0.25 ± 0.00 ^a	0.25 ± 0.00 ^a	0.25 ± 0.00 ^a	0.45 ± 0.01 ^b	0.30 ± 0.01 ^a	0.54 ± 0.02 ^b	0.36 ± 0.01 ^a	0.54 ± 0.02 ^b	0.59 ± 0.03 ^b	0.22 ± 0.00 ^a	0.58 ± 0.00 ^b	0.42 ± 0.01 ^b	0.58 ± 0.00 ^b	0.46 ± 0.02 ^c				
37:0	0.55 ± 0.01 ^a	0.51 ± 0.00 ^a	0.51 ± 0.00 ^a	0.73 ± 0.01 ^c	0.61 ± 0.01 ^a	0.87 ± 0.02 ^b	0.67 ± 0.00 ^a	0.87 ± 0.02 ^b	1.02 ± 0.01 ^c	0.51 ± 0.00 ^a	0.73 ± 0.01 ^b	0.73 ± 0.01 ^b	0.73 ± 0.01 ^b	0.85 ± 0.02 ^c				
38:0	7.16 ± 0.04 ^a	6.27 ± 0.05 ^b	6.27 ± 0.05 ^b	8.99 ± 0.12 ^c	7.63 ± 0.05 ^a	9.18 ± 0.27 ^b	7.59 ± 0.08 ^a	9.18 ± 0.27 ^b	11.46 ± 0.23 ^c	6.79 ± 0.10 ^a	6.76 ± 0.15 ^a	7.97 ± 0.00 ^b	6.76 ± 0.15 ^a	10.13 ± 0.12 ^d				
38:1	2.86 ± 0.03 ^a	2.74 ± 0.05 ^a	2.74 ± 0.05 ^a	3.82 ± 0.07 ^b	3.26 ± 0.04 ^a	3.99 ± 0.07 ^b	3.25 ± 0.04 ^a	3.99 ± 0.07 ^b	4.93 ± 0.02 ^c	2.72 ± 0.03 ^a	2.81 ± 0.02 ^a	3.26 ± 0.04 ^b	2.81 ± 0.02 ^a	3.99 ± 0.01 ^c				
38:2	0.82 ± 0.01 ^a	0.77 ± 0.02 ^a	0.77 ± 0.02 ^a	1.01 ± 0.02 ^b	0.93 ± 0.02 ^a	1.10 ± 0.00 ^{ab}	0.92 ± 0.00 ^a	1.10 ± 0.00 ^{ab}	1.38 ± 0.00 ^b	0.78 ± 0.00 ^a	0.76 ± 0.00 ^a	0.92 ± 0.00 ^b	0.76 ± 0.00 ^a	1.14 ± 0.01 ^c				
40:0	5.70 ± 0.04 ^a	4.83 ± 0.11 ^b	4.83 ± 0.11 ^b	5.02 ± 0.06 ^{bc}	5.3 ± 0.06 ^c	4.66 ± 0.07 ^b	4.83 ± 0.05 ^b	4.66 ± 0.07 ^b	6.21 ± 0.34 ^c	5.94 ± 0.04 ^a	4.86 ± 0.08 ^a	5.11 ± 0.04 ^c	4.86 ± 0.08 ^a	6.86 ± 0.01 ^d				
40:1	1.68 ± 0.05 ^a	1.48 ± 0.00 ^b	1.48 ± 0.00 ^b	1.52 ± 0.02 ^b	1.64 ± 0.00 ^a	1.65 ± 0.04 ^b	1.67 ± 0.03 ^b	1.65 ± 0.04 ^b	2.13 ± 0.07 ^a	1.56 ± 0.01 ^a	1.38 ± 0.00 ^b	1.40 ± 0.02 ^b	1.38 ± 0.00 ^b	1.83 ± 0.00 ^c				
42:0	2.38 ± 0.02 ^a	2.13 ± 0.02 ^b	2.13 ± 0.02 ^b	2.30 ± 0.01 ^a	2.68 ± 0.07 ^a	2.29 ± 0.08 ^c	2.42 ± 0.05 ^b	2.29 ± 0.08 ^c	2.82 ± 0.02 ^a	2.19 ± 0.00 ^a	2.13 ± 0.03 ^b	1.99 ± 0.03 ^b	2.13 ± 0.03 ^b	2.42 ± 0.00 ^c				
42:1	1.48 ± 0.03 ^a	1.74 ± 0.18 ^b	1.74 ± 0.18 ^b	1.54 ± 0.10 ^b	2.02 ± 0.06 ^a	1.50 ± 0.13 ^c	1.86 ± 0.20 ^b	1.50 ± 0.13 ^c	1.88 ± 0.17 ^b	1.83 ± 0.09 ^a	1.47 ± 0.07 ^b	1.43 ± 0.03 ^b	1.47 ± 0.07 ^b	1.65 ± 0.00 ^c				
42:2	1.24 ± 0.01 ^a	1.06 ± 0.01 ^b	1.06 ± 0.01 ^b	1.02 ± 0.03 ^b	1.42 ± 0.04 ^a	0.94 ± 0.03 ^c	1.13 ± 0.02 ^b	0.94 ± 0.03 ^c	1.14 ± 0.05 ^b	1.17 ± 0.02 ^a	0.94 ± 0.05 ^{bc}	0.82 ± 0.00 ^b	0.94 ± 0.05 ^{bc}	1.00 ± 0.01 ^c				
44:0	2.84 ± 0.02 ^a	2.44 ± 0.03 ^b	2.44 ± 0.03 ^b	1.55 ± 0.01 ^c	1.69 ± 0.02 ^a	1.67 ± 0.02 ^a	1.32 ± 0.04 ^b	1.67 ± 0.02 ^a	0.95 ± 0.06 ^c	3.47 ± 0.05 ^a	2.54 ± 0.06 ^b	2.36 ± 0.07 ^c	2.54 ± 0.06 ^b	2.42 ± 0.03 ^{bc}				
44:1	1.18 ± 0.02 ^a	1.04 ± 0.03 ^a	1.04 ± 0.03 ^a	0.78 ± 0.02 ^b	1.26 ± 0.03 ^a	0.67 ± 0.02 ^b	0.96 ± 0.04 ^b	0.67 ± 0.02 ^b	0.66 ± 0.06 ^c	1.13 ± 0.02 ^a	0.82 ± 0.00 ^b	0.67 ± 0.02 ^b	0.82 ± 0.00 ^b	0.72 ± 0.02 ^{bc}				
44:2	2.23 ± 0.04 ^a	1.98 ± 0.04 ^b	1.98 ± 0.04 ^b	1.19 ± 0.00 ^c	2.45 ± 0.03 ^a	1.37 ± 0.05 ^c	1.90 ± 0.02 ^b	1.37 ± 0.05 ^c	1.41 ± 0.09 ^c	2.15 ± 0.02 ^a	1.59 ± 0.05 ^b	1.35 ± 0.01 ^c	1.59 ± 0.05 ^b	1.41 ± 0.00 ^{bc}				
46:0	4.98 ± 0.15 ^a	5.08 ± 0.04 ^a	5.08 ± 0.04 ^a	2.79 ± 0.08 ^b	1.70 ± 0.02 ^a	0.88 ± 0.02 ^c	1.38 ± 0.05 ^b	0.88 ± 0.02 ^c	0.80 ± 0.05 ^c	5.45 ± 0.09 ^a	4.66 ± 0.25 ^b	4.37 ± 0.17 ^c	4.66 ± 0.25 ^b	4.44 ± 0.05 ^{bc}				
46:1	2.84 ± 0.08 ^a	2.43 ± 0.09 ^b	2.43 ± 0.09 ^b	1.27 ± 0.02 ^c	2.72 ± 0.11 ^a	1.42 ± 0.09 ^c	2.18 ± 0.05 ^b	1.42 ± 0.09 ^c	1.20 ± 0.10 ^d	2.95 ± 0.08 ^a	2.00 ± 0.01 ^b	1.59 ± 0.01 ^c	2.00 ± 0.01 ^b	1.44 ± 0.03 ^c				
46:2	1.48 ± 0.00 ^a	3.08 ± 0.31 ^b	3.08 ± 0.31 ^b	2.81 ± 0.00 ^b	2.84 ± 0.03 ^a	2.41 ± 0.09 ^c	3.50 ± 0.20 ^b	2.41 ± 0.09 ^c	2.42 ± 0.56 ^c	2.31 ± 0.04 ^a	2.33 ± 0.01 ^a	2.24 ± 0.03 ^a	2.33 ± 0.01 ^a	2.01 ± 0.04 ^b				
48:0	2.64 ± 0.11 ^a	3.30 ± 0.00 ^b	3.30 ± 0.00 ^b	2.75 ± 0.03 ^b	1.31 ± 0.01 ^a	0.68 ± 0.03 ^c	1.04 ± 0.01 ^b	0.68 ± 0.03 ^c	0.57 ± 0.01 ^d	2.49 ± 0.02 ^a	2.49 ± 0.02 ^a	2.04 ± 0.03 ^b	2.49 ± 0.02 ^a	2.28 ± 0.06 ^c				
48:1	3.54 ± 0.06 ^a	3.12 ± 0.01 ^b	3.12 ± 0.01 ^b	1.57 ± 0.00 ^c	3.50 ± 0.02 ^a	1.68 ± 0.00 ^c	2.60 ± 0.02 ^b	1.68 ± 0.00 ^c	1.21 ± 0.05 ^d	3.54 ± 0.13 ^a	2.71 ± 0.10 ^b	2.08 ± 0.00 ^c	2.71 ± 0.10 ^b	1.62 ± 0.02 ^d				
48:2	2.36 ± 0.01 ^a	2.08 ± 0.00 ^b	2.08 ± 0.00 ^b	1.35 ± 0.00 ^d	2.48 ± 0.00 ^a	1.18 ± 0.03 ^c	1.89 ± 0.02 ^b	1.18 ± 0.03 ^c	0.87 ± 0.08 ^d	2.37 ± 0.04 ^a	1.66 ± 0.02 ^b	1.24 ± 0.03 ^c	1.66 ± 0.02 ^b	0.97 ± 0.00 ^d				
48:3	0.24 ± 0.00 ^a	0.21 ± 0.00 ^a	0.21 ± 0.00 ^a	0.13 ± 0.01 ^b	0.27 ± 0.01 ^a	0.13 ± 0.01 ^b	0.19 ± 0.01 ^b	0.13 ± 0.01 ^b	0.09 ± 0.01 ^d	0.23 ± 0.00 ^a	0.16 ± 0 ^{0abb}	0.13 ± 0.00 ^b	0.16 ± 0 ^{0abb}	0.09 ± 0.00 ^c				
50:0	1.75 ± 0.09 ^a	3.00 ± 0.08 ^b	3.00 ± 0.08 ^b	1.65 ± 0.02 ^a	1.12 ± 0.01 ^a	0.60 ± 0.03 ^c	0.96 ± 0.04 ^b	0.60 ± 0.03 ^c	0.45 ± 0.01 ^d	1.70 ± 0.03 ^a	1.86 ± 0.28 ^{bc}	1.34 ± 0.06 ^b	1.86 ± 0.28 ^{bc}	2.00 ± 0.08 ^c				
50:1	5.65 ± 0.38 ^a	5.64 ± 0.07 ^a	5.64 ± 0.07 ^a	3.07 ± 0.05 ^b	5.43 ± 0.23 ^a	2.81 ± 0.09 ^c	4.43 ± 0.01 ^b	2.81 ± 0.09 ^c	1.84 ± 0.07 ^d	6.50 ± 0.20 ^a	4.99 ± 0.10 ^b	3.65 ± 0.01 ^c	4.99 ± 0.10 ^b	2.84 ± 0.07 ^d				
50:2	3.57 ± 0.07 ^a	3.02 ± 0.02 ^b	3.02 ± 0.02 ^b	1.47 ± 0.00 ^c	3.56 ± 0.09 ^a	1.70 ± 0.04 ^c	2.68 ± 0.01 ^b	1.70 ± 0.04 ^c	1.08 ± 0.02 ^d	3.33 ± 0.12 ^a	2.52 ± 0.03 ^b	1.83 ± 0.01 ^c	2.52 ± 0.03 ^b	1.42 ± 0.04 ^d				
50:3	1.03 ± 0.00 ^a	0.88 ± 0.03 ^b	0.88 ± 0.03 ^b	0.42 ± 0.01 ^c	1.06 ± 0.04 ^a	0.55 ± 0.01 ^c	0.88 ± 0.01 ^b	0.55 ± 0.01 ^c	0.35 ± 0.01 ^d	0.93 ± 0.01 ^a	0.70 ± 0.02 ^b	0.52 ± 0.00 ^c	0.70 ± 0.02 ^b	0.36 ± 0.01 ^d				
50:4	0.14 ± 0.01 ^a	0.13 ± 0.00 ^a	0.13 ± 0.00 ^a	0.08 ± 0.00 ^b	0.16 ± 0.01 ^a	0.07 ± 0.00 ^b	0.13 ± 0.00 ^a	0.07 ± 0.00 ^b	0.05 ± 0.00 ^b	0.10 ± 0.00 ^{ab}	0.10 ± 0.00 ^{ab}	0.07 ± 0.00 ^b	0.10 ± 0.00 ^{ab}	0.05 ± 0.00 ^b				
52:0	0.40 ± 0.01 ^a	0.76 ± 0.01 ^b	0.76 ± 0.01 ^b	0.51 ± 0.01 ^{bc}	0.31 ± 0.01 ^a	0.21 ± 0.02 ^b	0.29 ± 0.01 ^a	0.21 ± 0.02 ^b	0.15 ± 0.02 ^c	0.41 ± 0.01 ^a	0.45 ± 0.08 ^a	0.31 ± 0.02 ^b	0.45 ± 0.08 ^a	0.50 ± 0.01 ^c				
52:1	1.80 ± 0.02 ^a	1.67 ± 0.12 ^b	1.67 ± 0.12 ^b	1.08 ± 0.00 ^c	1.66 ± 0.04 ^a	0.92 ± 0.05 ^c	1.38 ± 0.06 ^b	0.92 ± 0.05 ^c	0.6 ± 0.04 ^d	1.79 ± 0.02 ^a	1.45 ± 0.06 ^b	1.05 ± 0.08 ^c	1.45 ± 0.06 ^b	0.89 ± 0.01 ^d				
52:2	5.73 ± 0.36 ^a	5.49 ± 0.11 ^b	5.49 ± 0.11 ^b	2.71 ± 0.19 ^c	6.63 ± 0.05 ^a	3.13 ± 0.02 ^c	5.08 ± 0.22 ^b	3.13 ± 0.02 ^c	1.94 ± 0.01 ^d	5.48 ± 0.33 ^a	4.41 ± 0.04 ^b	2.99 ± 0.12 ^c	4.41 ± 0.04 ^b	2.16 ± 0.02 ^d				
52:3	0.96 ± 0.01 ^a	0.91 ± 0.01 ^a	0.91 ± 0.01 ^a	0.59 ± 0.00 ^b	1.09 ± 0.00 ^a	0.52 ± 0.02 ^c	0.83 ± 0.01 ^b	0.52 ± 0.02 ^c	0.33 ± 0.00 ^d	0.95 ± 0.02 ^a	0.70 ± 0.00 ^b	0.51 ± 0.01 ^c	0.70 ± 0.00 ^b	0.35 ± 0.03 ^d				
52:4	0.17 ± 0.01 ^a	0.15 ± 0.01 ^a	0.15 ± 0.01 ^a	0.08 ± 0.00 ^b	0.19 ± 0.00 ^a	0.10 ± 0.00 ^b	0.15 ± 0.00 ^{ab}	0.10 ± 0.00 ^b	0.06 ± 0.00 ^c	0.16 ± 0.00 ^a	0.12 ± 0.01 ^b	0.09 ± 0.00 ^{bc}	0.12 ± 0.01 ^b	0.06 ± 0.00 ^c				
54:1	0.77 ± 0.04 ^a	0.78 ± 0.02 ^a	0.78 ± 0.02 ^a	0.56 ± 0.03 ^b	0.74 ± 0.00 ^a	0.44 ± 0.03 ^b	0.68 ± 0.00 ^a	0.44 ± 0.03 ^b	0.29 ± 0.05 ^c	0.72 ± 0.02 ^a	0.61 ± 0.04 ^{ab}	0.53 ± 0.05 ^b	0.61 ± 0.04 ^{ab}	0.42 ± 0.01 ^c				
54:2	1.17 ± 0.01 ^a	1.06 ± 0.01 ^a	1.06 ± 0.01 ^a	0.6														

Table 4. Triglyceride in residue of each fraction¹

Triglyceride	AMF						25 L						25 S					
	Room temperature (°C)		Distilling temperature (°C)		Room temperature (°C)		Distilling temperature (°C)		Room temperature (°C)		Distilling temperature (°C)		Room temperature (°C)		Distilling temperature (°C)			
	180	200	200	220	180	200	180	200	180	200	180	200	180	200	180	200		
26:0	0.02 ± 0.00 ^a	0.01 ± 0.00 ^a	0.00 ± 0.00 ^b	0.00 ± 0.00 ^b	0.02 ± 0.00 ^a	0.00 ± 0.00 ^b	0.00 ± 0.00 ^b	0.00 ± 0.00 ^b	0.02 ± 0.00 ^a	0.00 ± 0.00 ^b	0.00 ± 0.00 ^b	0.00 ± 0.00 ^b	0.00 ± 0.00 ^b	0.00 ± 0.00 ^b	0.00 ± 0.00 ^b	0.00 ± 0.00 ^b		
28:0	0.06 ± 0.00 ^a	0.03 ± 0.00 ^b	0.00 ± 0.00 ^c	0.00 ± 0.00 ^c	0.07 ± 0.00 ^a	0.02 ± 0.00 ^b	0.00 ± 0.00 ^b	0.00 ± 0.00 ^b	0.05 ± 0.00 ^a	0.00 ± 0.00 ^b	0.00 ± 0.00 ^b	0.00 ± 0.00 ^b	0.01 ± 0.00 ^b	0.00 ± 0.00 ^b	0.00 ± 0.00 ^b	0.00 ± 0.00 ^c		
30:0	0.65 ± 0.01 ^a	0.45 ± 0.01 ^b	0.08 ± 0.00 ^c	0.10 ± 0.00 ^c	0.75 ± 0.00 ^a	0.44 ± 0.01 ^b	0.44 ± 0.01 ^b	0.44 ± 0.01 ^b	0.61 ± 0.00 ^a	0.10 ± 0.00 ^c	0.04 ± 0.00 ^d	0.04 ± 0.00 ^d	0.29 ± 0.01 ^b	0.1 ± 0.00 ^c	0.05 ± 0.00 ^d	0.05 ± 0.00 ^d		
32:0	1.16 ± 0.01 ^a	0.97 ± 0.03 ^b	0.31 ± 0.01 ^c	0.39 ± 0.01 ^d	1.33 ± 0.02 ^a	1.05 ± 0.03 ^b	1.05 ± 0.03 ^b	1.05 ± 0.03 ^b	1.33 ± 0.02 ^a	0.45 ± 0.01 ^c	0.18 ± 0.00 ^d	0.18 ± 0.00 ^d	0.78 ± 0.03 ^b	0.42 ± 0.01 ^c	0.17 ± 0.00 ^d	0.17 ± 0.00 ^d		
34:0	4.26 ± 0.08 ^a	3.78 ± 0.01 ^b	1.93 ± 0.02 ^c	2.26 ± 0.09 ^d	4.77 ± 0.06 ^a	4.23 ± 0.01 ^b	4.23 ± 0.01 ^b	4.23 ± 0.01 ^b	4.77 ± 0.06 ^a	2.77 ± 0.05 ^c	1.47 ± 0.03 ^d	1.47 ± 0.03 ^d	3.38 ± 0.01 ^b	2.46 ± 0.06 ^c	1.06 ± 0.01 ^d	1.06 ± 0.01 ^d		
34:1	1.15 ± 0.00 ^a	1.02 ± 0.03 ^a	0.49 ± 0.01 ^b	0.58 ± 0.00 ^c	1.29 ± 0.02 ^a	1.15 ± 0.03 ^b	1.15 ± 0.03 ^b	1.15 ± 0.03 ^b	1.29 ± 0.02 ^a	0.68 ± 0.01 ^c	0.37 ± 0.00 ^d	0.37 ± 0.00 ^d	1.04 ± 0.01 ^a	0.67 ± 0.00 ^b	0.27 ± 0.00 ^c	0.27 ± 0.00 ^c		
35:0	0.20 ± 0.01 ^a	0.19 ± 0.00 ^a	0.11 ± 0.00 ^b	0.12 ± 0.00 ^b	0.22 ± 0.00 ^a	0.20 ± 0.00 ^b	0.20 ± 0.00 ^b	0.20 ± 0.00 ^b	0.22 ± 0.00 ^a	0.14 ± 0.00 ^b	0.09 ± 0.00 ^c	0.09 ± 0.00 ^c	0.16 ± 0.00 ^a	0.13 ± 0.00 ^a	0.06 ± 0.00 ^b	0.06 ± 0.00 ^b		
36:0	9.16 ± 0.01 ^a	8.39 ± 0.13 ^b	6.00 ± 0.15 ^c	6.27 ± 0.14 ^c	10.22 ± 0.05 ^a	9.73 ± 0.03 ^b	9.73 ± 0.03 ^b	9.73 ± 0.03 ^b	10.22 ± 0.05 ^a	8.08 ± 0.07 ^c	5.57 ± 0.02 ^d	5.57 ± 0.02 ^d	8.38 ± 0.09 ^a	7.09 ± 0.04 ^b	3.86 ± 0.09 ^c	3.86 ± 0.09 ^c		
36:1	1.14 ± 0.01 ^a	1.13 ± 0.03 ^a	0.79 ± 0.02 ^b	0.77 ± 0.02 ^b	1.37 ± 0.07 ^a	1.30 ± 0.02 ^a	1.30 ± 0.02 ^a	1.30 ± 0.02 ^a	1.37 ± 0.07 ^a	1.03 ± 0.01 ^b	0.69 ± 0.01 ^c	0.69 ± 0.01 ^c	1.10 ± 0.02 ^a	0.93 ± 0.01 ^b	0.46 ± 0.00 ^c	0.46 ± 0.00 ^c		
36:2	0.25 ± 0.00 ^a	0.25 ± 0.00 ^a	0.16 ± 0.00 ^b	0.16 ± 0.01 ^b	0.30 ± 0.01 ^a	0.28 ± 0.00 ^a	0.28 ± 0.00 ^a	0.28 ± 0.00 ^a	0.30 ± 0.01 ^a	0.22 ± 0.00 ^b	0.15 ± 0.00 ^c	0.15 ± 0.00 ^c	0.22 ± 0.00 ^a	0.23 ± 0.01 ^a	0.10 ± 0.00 ^b	0.10 ± 0.00 ^b		
37:0	0.55 ± 0.01 ^a	0.51 ± 0.00 ^a	0.42 ± 0.02 ^b	0.41 ± 0.01 ^b	0.61 ± 0.01 ^a	0.60 ± 0.01 ^a	0.60 ± 0.01 ^a	0.60 ± 0.01 ^a	0.61 ± 0.01 ^a	0.53 ± 0.00 ^b	0.4 ± 0.01 ^c	0.4 ± 0.01 ^c	0.51 ± 0.00 ^a	0.47 ± 0.01 ^a	0.29 ± 0.01 ^b	0.29 ± 0.01 ^b		
38:0	7.16 ± 0.04 ^a	6.65 ± 0.04 ^b	6.01 ± 0.03 ^c	5.8 ± 0.06 ^c	7.63 ± 0.05 ^a	7.67 ± 0.13 ^a	7.67 ± 0.13 ^a	7.67 ± 0.13 ^a	7.63 ± 0.05 ^a	7.34 ± 0.19 ^b	5.91 ± 0.00 ^c	5.91 ± 0.00 ^c	6.79 ± 0.1 ^a	6.83 ± 0.15 ^a	4.56 ± 0.03 ^c	4.56 ± 0.03 ^c		
38:1	2.86 ± 0.03 ^a	2.81 ± 0.14 ^a	2.46 ± 0.01 ^b	2.42 ± 0.03 ^b	3.26 ± 0.04 ^{ab}	3.36 ± 0.01 ^a	3.36 ± 0.01 ^a	3.36 ± 0.01 ^a	3.26 ± 0.04 ^{ab}	3.15 ± 0.01 ^b	2.51 ± 0.04 ^c	2.51 ± 0.04 ^c	2.72 ± 0.03 ^a	2.84 ± 0.01 ^a	1.78 ± 0.00 ^b	1.78 ± 0.00 ^b		
38:2	0.82 ± 0.01 ^a	0.79 ± 0.02 ^a	0.68 ± 0.01 ^b	0.66 ± 0.02 ^b	0.93 ± 0.02 ^a	0.95 ± 0.02 ^a	0.95 ± 0.02 ^a	0.95 ± 0.02 ^a	0.93 ± 0.02 ^a	0.89 ± 0.01 ^{ab}	0.70 ± 0.01 ^b	0.70 ± 0.01 ^b	0.78 ± 0.00 ^a	0.80 ± 0.02 ^a	0.50 ± 0.00 ^b	0.50 ± 0.00 ^b		
40:0	5.70 ± 0.04 ^a	5.29 ± 0.05 ^b	5.37 ± 0.06 ^b	5.05 ± 0.12 ^c	5.58 ± 0.09 ^a	5.82 ± 0.07 ^b	5.82 ± 0.07 ^b	5.82 ± 0.07 ^b	5.58 ± 0.09 ^a	5.85 ± 0.01 ^b	5.38 ± 0.02 ^c	5.38 ± 0.02 ^c	5.94 ± 0.04 ^a	6.10 ± 0.03 ^a	6.15 ± 0.00 ^b	6.15 ± 0.00 ^b		
40:1	1.68 ± 0.05 ^a	1.66 ± 0.04 ^a	1.63 ± 0.03 ^a	1.56 ± 0.06 ^b	1.93 ± 0.01 ^a	1.97 ± 0.01 ^a	1.97 ± 0.01 ^a	1.97 ± 0.01 ^a	1.93 ± 0.01 ^a	1.99 ± 0.01 ^a	1.80 ± 0.04 ^b	1.80 ± 0.04 ^b	1.56 ± 0.01 ^a	1.66 ± 0.00 ^b	1.65 ± 0.02 ^b	1.65 ± 0.02 ^b		
40:2	2.38 ± 0.02 ^a	2.31 ± 0.02 ^{ab}	2.27 ± 0.05 ^b	2.12 ± 0.07 ^c	2.68 ± 0.07 ^a	2.68 ± 0.05 ^a	2.68 ± 0.05 ^a	2.68 ± 0.05 ^a	2.68 ± 0.07 ^a	2.82 ± 0.00 ^b	2.55 ± 0.05 ^c	2.55 ± 0.05 ^c	2.19 ± 0.00 ^a	2.28 ± 0.02 ^a	1.85 ± 0.03 ^b	1.85 ± 0.03 ^b		
42:1	1.48 ± 0.03 ^a	1.77 ± 0.02 ^b	1.94 ± 0.07 ^c	1.90 ± 0.16 ^c	2.02 ± 0.06 ^a	1.98 ± 0.06 ^a	1.98 ± 0.06 ^a	1.98 ± 0.06 ^a	2.02 ± 0.06 ^a	2.48 ± 0.14 ^{ab}	2.23 ± 0.10 ^b	2.23 ± 0.10 ^b	1.83 ± 0.09 ^a	1.94 ± 0.14 ^b	1.92 ± 0.01 ^b	1.80 ± 0.23 ^a		
42:2	1.24 ± 0.01 ^a	1.21 ± 0.07 ^a	1.29 ± 0.03 ^b	1.24 ± 0.02 ^b	1.42 ± 0.04 ^a	1.46 ± 0.04 ^{ab}	1.46 ± 0.04 ^{ab}	1.46 ± 0.04 ^{ab}	1.42 ± 0.04 ^a	1.56 ± 0.02 ^b	1.55 ± 0.02 ^b	1.55 ± 0.02 ^b	1.17 ± 0.02	1.21 ± 0.01	1.26 ± 0.01	1.26 ± 0.02		
44:0	2.84 ± 0.02 ^a	2.77 ± 0.00 ^a	3.07 ± 0.10 ^b	3.03 ± 0.02 ^b	1.69 ± 0.02 ^a	1.74 ± 0.01 ^a	1.74 ± 0.01 ^a	1.74 ± 0.01 ^a	1.69 ± 0.02 ^a	1.96 ± 0.06 ^b	2.06 ± 0.08 ^b	2.06 ± 0.08 ^b	3.47 ± 0.05 ^a	3.38 ± 0.03 ^a	3.67 ± 0.02 ^b	4.05 ± 0.1 ^c		
44:1	1.18 ± 0.02	1.18 ± 0.05	1.22 ± 0.00	1.21 ± 0.05	1.26 ± 0.03 ^a	1.28 ± 0.01 ^a	1.28 ± 0.01 ^a	1.28 ± 0.01 ^a	1.26 ± 0.03 ^a	1.35 ± 0.02 ^{ab}	1.46 ± 0.01 ^b	1.46 ± 0.01 ^b	1.13 ± 0.02 ^a	1.22 ± 0.02 ^a	1.28 ± 0.00 ^c	1.40 ± 0.00 ^c		
44:2	2.23 ± 0.04 ^a	2.21 ± 0.06 ^a	2.46 ± 0.01 ^b	2.34 ± 0.08 ^{ab}	2.45 ± 0.03 ^a	2.57 ± 0.03 ^{ab}	2.57 ± 0.03 ^{ab}	2.57 ± 0.03 ^{ab}	2.45 ± 0.03 ^a	2.69 ± 0.00 ^b	2.99 ± 0.05 ^c	2.99 ± 0.05 ^c	2.15 ± 0.02 ^a	2.27 ± 0.01 ^a	2.45 ± 0.07 ^b	2.58 ± 0.02 ^c		
46:0	4.98 ± 0.15 ^a	5.31 ± 0.06 ^b	5.89 ± 0.19 ^c	6.27 ± 0.22 ^d	1.7 ± 0.02 ^{ab}	1.77 ± 0.06 ^{ab}	1.77 ± 0.06 ^{ab}	1.77 ± 0.06 ^{ab}	1.7 ± 0.02 ^{ab}	1.87 ± 0.01 ^b	2.22 ± 0.03 ^c	2.22 ± 0.03 ^c	5.45 ± 0.09 ^a	5.20 ± 0.27 ^b	5.49 ± 0.02 ^c	5.96 ± 0.11 ^c		
46:1	2.84 ± 0.08 ^a	2.90 ± 0.05 ^a	3.06 ± 0.01 ^b	2.99 ± 0.12 ^b	2.72 ± 0.11 ^a	2.99 ± 0.01 ^{ab}	2.99 ± 0.01 ^{ab}	2.99 ± 0.01 ^{ab}	2.72 ± 0.11 ^a	3.17 ± 0.1 ^b	3.84 ± 0.11 ^c	3.84 ± 0.11 ^c	2.95 ± 0.08 ^a	3.00 ± 0.00 ^a	3.32 ± 0.04 ^b	3.78 ± 0.10 ^c		
46:2	1.48 ± 0.00 ^a	2.05 ± 0.05 ^b	2.86 ± 0.13 ^c	2.07 ± 0.02 ^b	2.84 ± 0.03 ^a	2.25 ± 0.08 ^b	2.25 ± 0.08 ^b	2.25 ± 0.08 ^b	2.84 ± 0.03 ^a	2.71 ± 0.29 ^b	3.56 ± 0.05 ^c	3.56 ± 0.05 ^c	2.31 ± 0.04 ^a	2.12 ± 0.03 ^b	2.13 ± 0.04 ^b	3.09 ± 0.09 ^c		
48:0	2.64 ± 0.11 ^a	3.13 ± 0.27 ^b	3.50 ± 0.11 ^c	3.86 ± 0.47 ^d	1.31 ± 0.01 ^a	1.25 ± 0.03 ^a	1.25 ± 0.03 ^a	1.25 ± 0.03 ^a	1.31 ± 0.01 ^a	1.37 ± 0.05 ^a	1.61 ± 0.09 ^b	1.61 ± 0.09 ^b	2.49 ± 0.02 ^{ab}	2.4 ± 0.03 ^a	2.52 ± 0.07 ^b	2.87 ± 0.06 ^c		
48:1	3.54 ± 0.06 ^a	3.51 ± 0.02 ^a	3.98 ± 0.04 ^b	3.88 ± 0.05 ^b	3.50 ± 0.02 ^a	3.53 ± 0.01 ^a	3.53 ± 0.01 ^a	3.53 ± 0.01 ^a	3.50 ± 0.02 ^a	3.99 ± 0.01 ^b	4.46 ± 0.02 ^c	4.46 ± 0.02 ^c	3.54 ± 0.13 ^a	3.43 ± 0.38 ^a	4.06 ± 0.08 ^b	4.74 ± 0.15 ^c		
48:2	2.36 ± 0.01 ^a	2.32 ± 0.03 ^a	2.60 ± 0.00 ^b	2.61 ± 0.11 ^b	2.48 ± 0.00 ^a	2.65 ± 0.01 ^a	2.65 ± 0.01 ^a	2.65 ± 0.01 ^a	2.48 ± 0.00 ^a	2.9 ± 0.01 ^b	3.38 ± 0.01 ^c	3.38 ± 0.01 ^c	2.37 ± 0.04 ^a	2.43 ± 0.05 ^a	2.63 ± 0.00 ^b	3.11 ± 0.01 ^c		
48:3	0.24 ± 0.00	0.23 ± 0.01	0.27 ± 0.01	0.26 ± 0.00	0.27 ± 0.01 ^a	0.3 ± 0.01 ^a	0.3 ± 0.01 ^a	0.3 ± 0.01 ^a	0.27 ± 0.01 ^a	0.31 ± 0.01 ^a	0.36 ± 0.01 ^b	0.36 ± 0.01 ^b	0.23 ± 0.00 ^a	0.23 ± 0.00 ^a	0.25 ± 0.01 ^a	0.31 ± 0.01 ^b		
50:0	1.75 ± 0.09 ^a	2.53 ± 0.29 ^b	2.80 ± 0.13 ^c	3.32 ± 0.55 ^d	1.12 ± 0.01 ^a	1.23 ± 0.02 ^{ab}	1.23 ± 0.02 ^{ab}	1.23 ± 0.02 ^{ab}	1.12 ± 0.01 ^a	1.31 ± 0.00 ^b	1.54 ± 0.01 ^c	1.54 ± 0.01 ^c	1.70 ± 0.03 ^a	1.56 ± 0.01 ^b	1.63 ± 0.04 ^{ab}	1.92 ± 0.02 ^c		
50:1	5.65 ± 0.38 ^a	6.29 ± 0.03 ^b	7.07 ± 0.02 ^c	7.06 ± 0.09 ^c	5.43 ± 0.23 ^a	5.59 ± 0.22 ^b	5.59 ± 0.22 ^b	5.59 ± 0.22 ^b	5.43 ± 0.23 ^a	6.35 ± 0.19 ^c	7.02 ± 0.33 ^d	7.02 ± 0.33 ^d	6.50 ± 0.20 ^a	6.6 ± 0.17 ^a	6.17 ± 0.26 ^b	8.11 ± 0.31 ^c		
50:2	3.57 ± 0.07 ^a	3.34 ± 0.01 ^b	3.8 ± 0.01 ^c	3.68 ± 0.16 ^b	3.56 ± 0.09 ^a	3.86 ± 0.01 ^b	3.86 ± 0.01 ^b	3.86 ± 0.01 ^b	3.56 ± 0.09 ^a	4.12 ± 0.01 ^b	4.60 ± 0.02 ^c	4.60 ± 0.02 ^c	3.33 ± 0.12 ^a	3.55 ± 0.13 ^{ab}	3.88 ± 0.02 ^b	4.65 ± 0.06 ^c		
50:3	1.03 ± 0.00 ^a	0.97 ± 0.03 ^a	1.12 ± 0.01 ^b	1.12 ± 0.02 ^b	1.06 ± 0.04 ^a	1.14 ± 0.05 ^a	1.14 ± 0.05 ^a	1.14 ± 0.05 ^a	1.06 ± 0.04 ^a	1.25 ± 0.09 ^b	1.51 ± 0.03 ^c	1.51 ± 0.03 ^c	0.93 ± 0.01 ^a	1.02 ± 0.00 ^a	1.06 ± 0.02 ^a	1.33 ± 0.01 ^b		
50:4	0.14 ± 0.01	0.14 ± 0.00	0.16 ± 0.00	0.17 ± 0.00	0.16 ± 0.01 ^a	0.18 ± 0.01 ^a	0.18 ± 0.01 ^a	0.18 ± 0.01 ^a	0.16 ± 0.01 ^a	0.19 ± 0.00 ^b	0.21 ± 0.01 ^b	0.21 ± 0.01 ^b	0.13 ± 0.01 ^a	0.15 ± 0.00 ^a	0.16 ± 0.01 ^a	0.19 ± 0.00 ^b		
52:0	0.40 ± 0.01 ^a	0.64 ± 0.1 ^b	0.72 ± 0.07 ^{bc}	0.83 ± 0.16 ^c	0.31 ± 0.01 ^a	0.32 ± 0.00 ^b	0.32 ± 0.00 ^b	0.32 ± 0.00 ^b	0.31 ± 0.01 ^a	0.37 ± 0.00 ^b	0.39 ± 0.00 ^b	0.39 ± 0.00 ^b	0.41 ± 0.01	0.38 ± 0.01	0.39 ± 0.02	0.43 ± 0.01		
52:1	1.8 ± 0.02 ^a	1.69 ± 0.03 ^a	2.06 ± 0.00 ^b	2.12 ± 0.04 ^b	1.66 ± 0.04 ^a	1.79 ± 0.04 ^{ab}	1.79 ± 0.04 ^{ab}	1.79 ± 0.04 ^{ab}	1.66 ± 0.04 ^a	1.93 ± 0.01 ^b	2.38 ± 0.11 ^c	2.38 ± 0.11 ^c	1.79 ±					

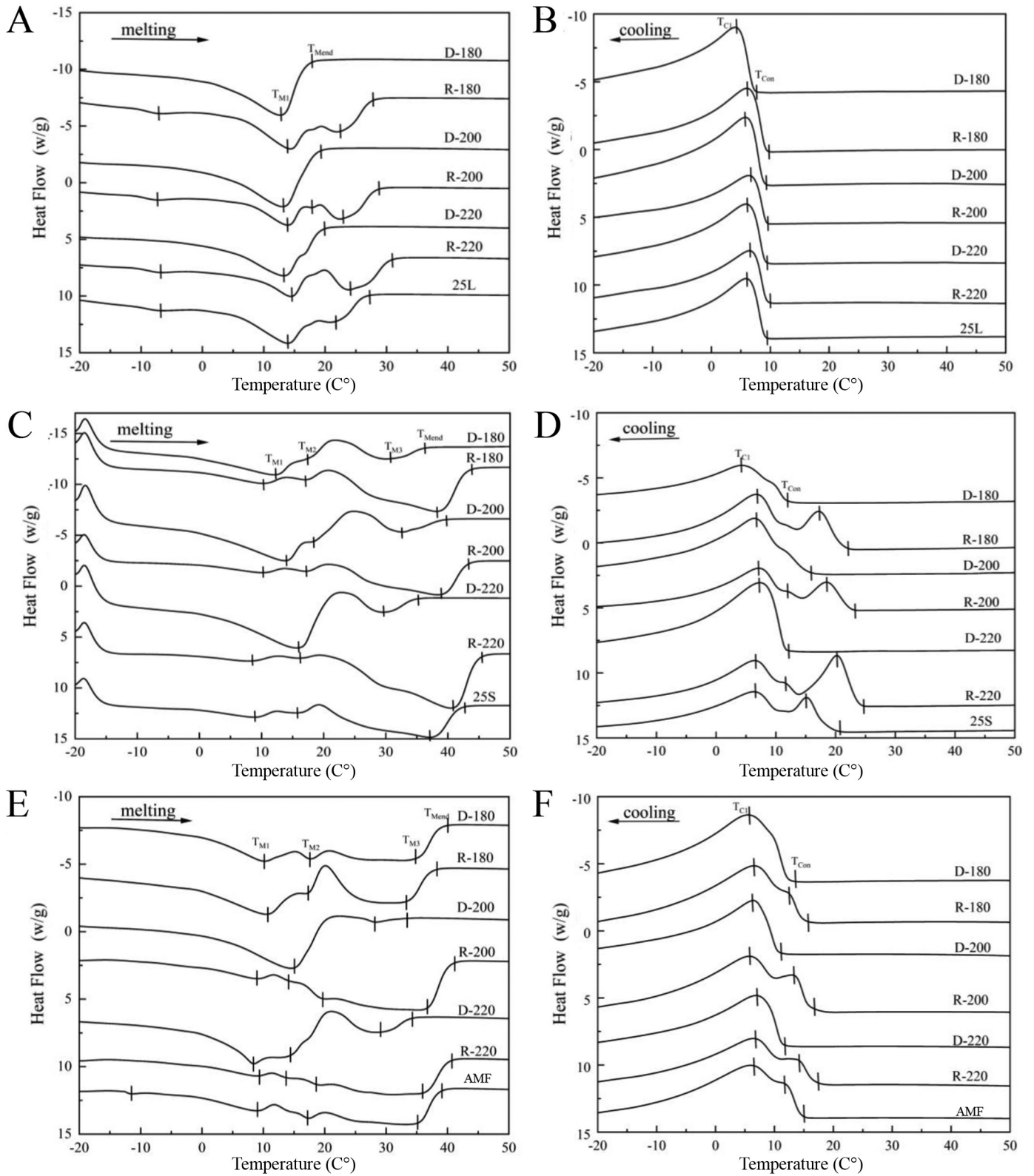


Figure 5. Differential scanning calorimeter crystallization-melting diagram of milk fat separation products, in which plots A, C, and E represent the melting curves of 25 L, 25 S, AMF, and their distilling products; plots B, D, and F represent the crystallization curves of 25 L, 25 S, AMF, and their distilling products. AMF = anhydrous milk fat; 25 L = liquid fraction at 25°C; 25 S = solid fraction at 25°C; D = distillate; R = residue

and $>50^{\circ}\text{C}$), corresponding with α , β' , and β crystals, respectively (Che Man et al., 1999). Therefore, we conjectured that the distillate was preferentially formed by α crystal in this research, while the residue was mixed by α and β crystals.

It was evident that the number of exothermic peaks in the crystallization curve was lower than the number of endothermic peaks in the melting curve (Figure 5). We detected several reasons for this phenomenon. First, the molecular chains of MF required some delay time before entering into the crystal lattice during crystallization; the degree of supercooling increased gradually with the ambient temperature decreased, leading to the low-melting-point component of substrate being crystallized, and the exothermic peaks appeared simultaneously (Márquez et al., 2013). Furthermore, the kind of FA in MF are diverse, with the melting point of TAG comprised of 3 SFA was higher than that of the TAG with one or 2 SFA, resulting in the inexact detection of absolute melting point of MF. Finally, the polymorphism apparent in MF indicates that there are different crystalline forms for one substance, producing α , β , and β' crystals under different conditions (Kaylegian and Lindsay, 1992; Wang et al., 2019). The crystals of MF showed the concomitant phenomenon of crystallization and melt with the increase of processing temperature. This might be caused by some TAG with poor thermal stability were first melted at the early stage in heating process, whereafter the remaining TAG were rearranged and recrystallized to a more stable crystal form, and melting occurred at a higher temperature (Wang et al., 2010).

Crystal Forms and Accumulation Patterns

Milk fat is composed of α , β' , and β crystals, the melting points of which are 65°C , 70°C , and 72°C , respectively (Van Aken and Visser, 2000). In the crystallization process, α crystal is produced at the first stage because of its unstable property, and it quickly transforms to β' and β crystals (ten Grotenhuis et al., 1999). Undoubtedly, the crystallizing characteristics of MF is showed by the crystal polymorphism, therefore, the crystal accumulation and morphology of MF are usually detected via the long- and short-spacing models of XRD (van Aken et al., 1999). Here, in the short-spacing model, α crystal corresponded with the diffraction peak near 4.15 \AA , the diffraction peaks around 4.2 \AA and 3.8 \AA all represented β' crystal, and the diffraction peak located at 4.60 \AA corresponded with β crystal (Szydłowska-Czerniak et al., 2005). As shown in graphs A, C, and F of Figure 6, we detected almost no diffraction peak in the curve of 25 L and its distilling products, which might have given rise to the

existence of these compounds as liquids, which were not able to crystallize at room temperature. However, the strong diffraction peaks at 3.80 \AA , 4.15 \AA , and 4.28 \AA were demonstrated in the distillates of 25 S and AMF, indicating that they were mixed α and β' crystals. In addition, the 25 S, AMF, and their residues all had diffraction peaks near 4.52 \AA and 4.56 \AA , indicating these compounds were mixed with α , β' , and β crystals. The height of diffraction peaks at 3.80 \AA , 4.28 \AA , and 4.58 \AA all rose apparently with the increase of distilling temperature in the residue of AMF and 25 S, however, they were observed a decrease in the distillate. These results showed that there were more β' crystal in the residues of AMF and 25 S.

The structure of chain length is formed by the TAG crystals, which is detected by the long-spacing model of XRD. It was reported that the accumulation pattern of TAG was a double-length structure (2L) when we detected diffraction peaks near 41 \AA and 14 \AA in the long-spacing model. Moreover, the crystal structure was determined to be a triple-length structure (3L) when the diffraction peaks were appeared near 61 \AA and 31 \AA (Sato, 2001, Haddad et al., 2010). In this study, 25 L, 25 S, and AMF all had diffraction peaks at 40.50 \AA , and the corresponding refraction peaks appeared near 13.70 \AA , indicating that these components were arranged as the 2L structure (Graphs B, D, and F of Figure 6). The long-spacing models of distillates and residues were similar to those of their distilling substrates, and the diffraction peak heights at 40.50 \AA and 13.70 \AA all decreased in the residues as the increase of distilling temperature. Furthermore, the low-intensity refraction peak at 29.44 \AA was only observed in AMF, 25 S, and their residues, and the height of refraction peak decreased during the distilling process. This was because the TAG of the abovementioned components was mixed by 2L and 3L structures at the early stage of the SPMD, and then the percentages of LMW- and MMW-TAG gradually decreased, resulting in that the accumulation pattern of TAG was transformed to a single 2L structure.

The height of diffraction peak in the residues was higher than those of the distillates at the same distilling temperature, in both the long- or short-spacing models, possibly because the degree of polymorphism in the distillate was lower than that of the residues. In addition, the height of diffraction peaks in the distilling products all decreased with the increase of distilling temperature. These phenomena indicated that the degree of polymorphism in the distilling products decreased during the distillation process, and the accumulation pattern of TAG was simultaneously transformed to a single 2L structure at the same time. Previous studies also reported a decrease in degree of freedom in MF, and

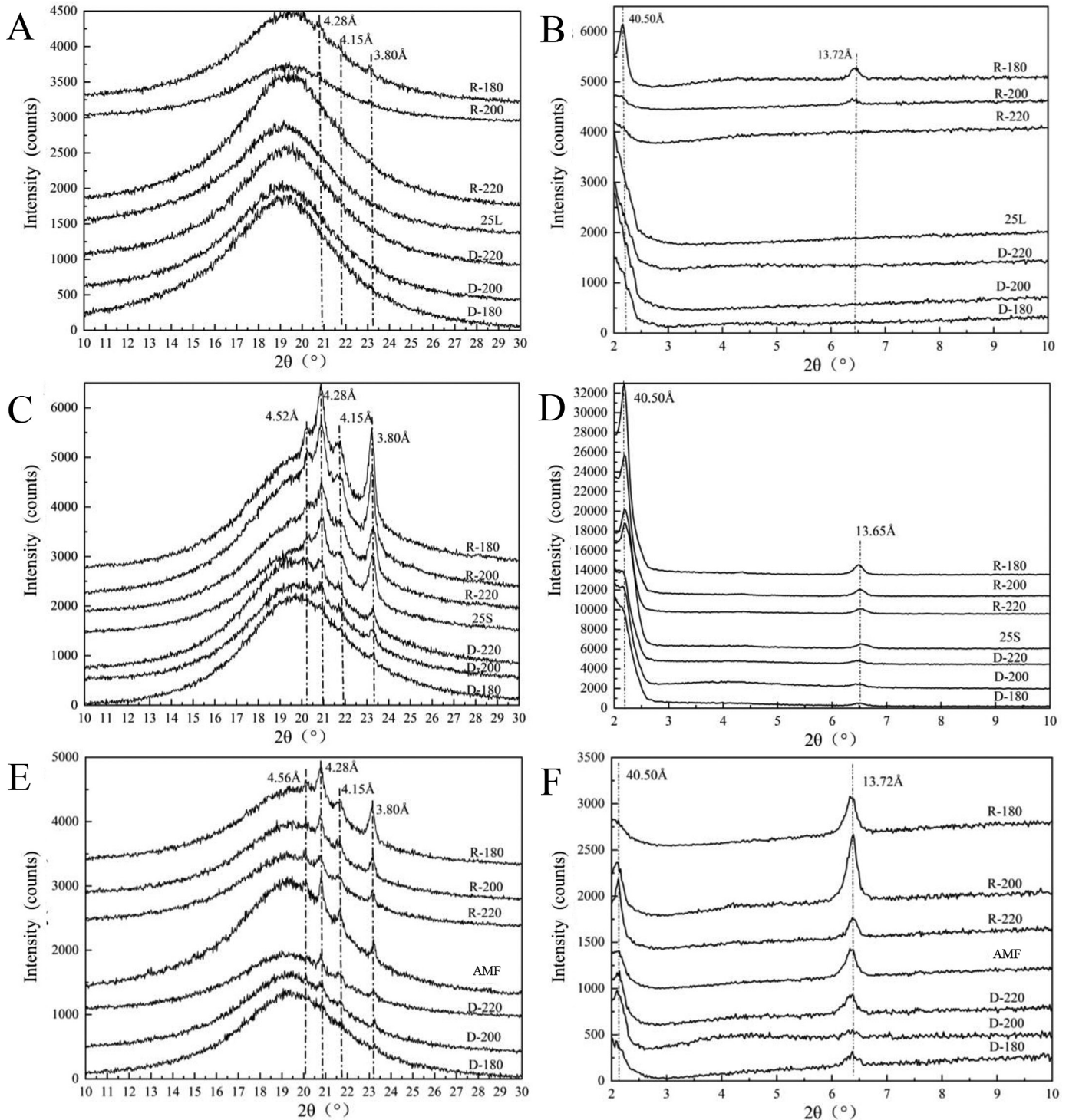


Figure 6. X-ray diffraction diagram of milk fat separation products, in which plots A, C, and E represent the crystal forms of 25 L, 25 S, AMF, and their distilling products, detected via short-spacing model; plots B, D, and F represent the accumulation patterns of 25 L, 25 S, AMF, and their distilling products, detected via long-spacing model. AMF = anhydrous milk fat; 25 L = liquid fraction at 25°C; 25 S = solid fraction at 25°C; D = distillate; R = residue.

the MF molecules moved slowly in the crystallization process, taking certain time to form a stable lattice. The transformation from α crystal to β crystal was a spontaneous process ($\delta G < 0$), which could only be accelerated or delayed rather than prevented by temperature and crystallization rate (Herrera et al., 1999), and this transformation was rapid while it was slow from β' crystal to β crystal. In addition, when TAG are mainly accumulated by 3L structure, the melting point of MF is higher and leads to a rough tasting product, while the properties of MF have a rigid structure and soft sense when the TAG are consisted with long-chain UFA and MC-SFA (Tietz and Hartel, 2000).

CONCLUSIONS

The percentages of SC-SFA, MC-SFA, LMW-, and MMW-TAG were higher in the distillate, and UFA and HMM-TAG were accumulated easily in the residue. Furthermore, the contents of FA and TAG both in 25 S and 25 L were affected obviously by the SPMD in comparison to those of AMF. There were no diffraction peaks in 25 L and its distilling products; the 25 S, AMF, and their distillates were constituted with α and β' crystals, and their residues were composed of α , β' , and β crystals. The accumulation patterns of 25 L, 25 S, AMF, and their distilling products all were 2L structure. Therefore, the combination of DF and SPMD had a more significant effect on the separation of MF when compared with the single fraction method, and these phenomena present a new approach for the separation of MF and provide some theoretical data for the MF in practical production.

ACKNOWLEDGMENTS

This work was funded by the National Key Research and Development Program of China (2021YFD2100700, 2017YFE0131800; Beijing, China), the Ningxia Key Research and Development Program (2021BEF02022; Yinchuan, China), the Inner Mongolia Science and Technology Program (2021GG0368; Hohhot, China), the Agricultural Science and Technology Innovation Program of the Institute of Food Science and Technology, and the Chinese Academy of Agricultural Sciences (CAAS-ASTIP-G2022-IFST-04; Beijing, China). Author contributions: NJ, SZ, and JLv: conceptualization and validation. HZ and XS: methodology. PZ, XW, and YW: software and investigation. XP, PZ, and YW: formal analysis. SZ and JLv: resources. HZ and XS: data curation, writing—original draft preparation, and visualization. HZ, YW, XS, NJ, SW, MLF and JLv: writing—review and editing. NJ and SZ: supervision. NJ, SZ, and JLv: project administration. NJ, SZ, and





JLv: funding acquisition. All authors have read and agreed to the published version of the manuscript. The authors have not stated any conflicts of interest.

REFERENCES

- Anankanbil, S., M. Larsen, M. Weisbjerg, and L. Wiking. 2018. Effects of variation in fatty acids and triglyceride composition on melting behavior in milk fat. *Milk Science International—Milchwissenschaft* 71:4–9.
- Arul, J., A. Boudreau, J. Makhlof, R. Tardi, and T. Bellavia. 1988. Fractionation of anhydrous milk fat by short-path distillation. *J. Am. Oil Chem. Soc.* 65:1642. <https://doi.org/10.1007/BF02912569>.
- Berti, J., N. R. Grosso, H. Fernandez, M. C. Pramparo, and M. F. Gayol. 2018. Sensory quality of milk fat with low cholesterol content fractionated by molecular distillation. *J. Sci. Food Agric.* 98:3478–3484. <https://doi.org/10.1002/jsfa.8866>.
- Bonomi, E. C., V. Luccas, and T. G. Kieckbusch. 2012. Characterization of the stearin obtained by thermal fractionation of anhydrous milk fat. *Procedia Eng.* 42:918–923. <https://doi.org/10.1016/j.proeng.2012.07.484>.
- Boudreau, A., and J. Arul. 1993. Cholesterol reduction and fat fractionation technologies for milk fat: An overview. *J. Dairy Sci.* 76:1772–1781. [https://doi.org/10.3168/jds.S0022-0302\(93\)77509-8](https://doi.org/10.3168/jds.S0022-0302(93)77509-8).
- Campos, R. J., J. W. Litwinenko, and A. G. Marangoni. 2003. Fractionation of milk fat by short-path distillation. *J. Dairy Sci.* 86:735–745. [https://doi.org/10.3168/jds.S0022-0302\(03\)73654-6](https://doi.org/10.3168/jds.S0022-0302(03)73654-6).
- Che Man, Y. B., T. Haryati, H. M. Ghazali, and B. A. Asbi. 1999. Composition and thermal profile of crude palm oil and its products. *J. Am. Oil Chem. Soc.* 76:237–242. <https://doi.org/10.1007/s11746-999-0224-y>.
- Deffense, E. 1993. Milk fat fractionation today: A review. *J. Am. Oil Chem. Soc.* 70:1193–1201. <https://doi.org/10.1007/BF02564225>.
- Fatouh, A. E., R. K. Singh, P. E. Koehler, G. A. Mahran, M. A. El-Ghandour, and A. E. Metwally. 2003. Chemical and thermal characteristics of buffalo butter oil fractions obtained by multi-step dry fractionation. *Lebensm. Wiss. Technol.* 36:483–496. [https://doi.org/10.1016/S0023-6438\(03\)00044-6](https://doi.org/10.1016/S0023-6438(03)00044-6).
- Gómez-Cortés, P., M. Juárez, and M. A. de la Fuente. 2018. Milk fatty acids and potential health benefits: An updated vision. *Trends Food Sci. Technol.* 81:1–9. <https://doi.org/10.1016/j.tifs.2018.08.014>.
- Haddad, I., M. Mozzon, R. Strabbioli, and N. G. Frega. 2010. Stereo-specific analysis of triacylglycerols in camel (*Camelus dromedarius*) milk fat. *Int. Dairy J.* 20:863–867. <https://doi.org/10.1016/j.idairyj.2010.06.006>.
- Herrera, M. L., M. de León Gatti, and R. W. Hartel. 1999. A kinetic analysis of crystallization of a milk fat model system. *Food Res. Int.* 32:289–298. [https://doi.org/10.1016/S0963-9969\(99\)00083-6](https://doi.org/10.1016/S0963-9969(99)00083-6).
- Jensen, R. G. 2002. The composition of bovine milk lipids: January 1995 to December 2000. *J. Dairy Sci.* 85:295–350. [https://doi.org/10.3168/jds.S0022-0302\(02\)74079-4](https://doi.org/10.3168/jds.S0022-0302(02)74079-4).
- Kaylegian, K. E., and R. C. Lindsay. 1992. Performance of selected milk fat fractions in cold-spreadable butter. *J. Dairy Sci.* 75:3307–3317. [https://doi.org/10.3168/jds.S0022-0302\(92\)78106-5](https://doi.org/10.3168/jds.S0022-0302(92)78106-5).
- Lohman, M. H., and R. W. Hartel. 1994. Effect of milk fat fractions on fat bloom in dark chocolate. *J. Am. Oil Chem. Soc.* 71:267–276. <https://doi.org/10.1007/BF02638052>.
- Lopez, C., C. Bourgaux, P. Lesieur, A. Riaublanc, and M. Ollivon. 2006. Milk fat and primary fractions obtained by dry fractionation: 1. Chemical composition and crystallisation properties. *Chem. Phys. Lipids* 144:17–33. <https://doi.org/10.1016/j.chemphyslip.2006.06.002>.
- Lopez, C., P. Lesieur, C. Bourgaux, G. Keller, and M. Ollivon. 2001. Thermal and structural behavior of milk fat. *J. Colloid Interface Sci.* 240:150–161. <https://doi.org/10.1006/jcis.2001.7664>.
- Małkowska, M., B. Staniewski, and J. Ziajka. 2021. Analyses of milk fat crystallization and milk fat fractions. *Int. J. Food Prop.* 24:325–336. <https://doi.org/10.1080/10942912.2021.1878217>.

- Márquez, A. L., M. P. Pérez, and J. R. Wagner. 2013. Solid fat content estimation by differential scanning calorimetry: Prior treatment and proposed correction. *J. Am. Oil Chem. Soc.* 90:467–473. <https://doi.org/10.1007/s11746-012-2190-z>.
- Mohan, M. S., T. F. O’Callaghan, P. Kelly, and S. A. Hogan. 2021. Milk fat: Opportunities, challenges, and innovation. *Crit. Rev. Food Sci. Nutr.* 61:2411–2443. <https://doi.org/10.1080/10408398.2020.1778631>.
- O’Shea, M., R. Devery, F. Lawless, K. Keogh, and C. Stanton. 2000. Enrichment of the conjugated linoleic acid content of bovine milk fat by dry fractionation. *Int. Dairy J.* 10:289–294. [https://doi.org/10.1016/S0958-6946\(00\)00049-2](https://doi.org/10.1016/S0958-6946(00)00049-2).
- Ransom-Painter, K. L., S. D. Williams, and R. W. Hartel. 1997. Incorporation of milk fat and milk fat fractions into compound coatings made from palm kernel oil. *J. Dairy Sci.* 80:2237–2248. [https://doi.org/10.3168/jds.S0022-0302\(97\)76172-1](https://doi.org/10.3168/jds.S0022-0302(97)76172-1).
- Sato, K. 2001. Crystallization behaviour of fats and lipids—A review. *Chem. Eng. Sci.* 56:2255–2265. [https://doi.org/10.1016/S0009-2509\(00\)00458-9](https://doi.org/10.1016/S0009-2509(00)00458-9).
- Si, X., H. Zhu, P. Zhu, Y. Wang, X. Pang, N. Ju, J. Lv, and S. Zhang. 2023. Triacylglycerol composition and thermodynamic profiles of fractions from dry fractionation of anhydrous milk fat. *J. Food Compos. Anal.* 115:104916. <https://doi.org/10.1016/j.jfca.2022.104916>.
- Silva, R. C., F. A. S. D. M. Soares, J. M. Maruyama, N. R. Dagozinho, Y. A. Silva, G. A. Calligaris, A. P. B. Ribeiro, L. P. Cardoso, and L. A. Gioielli. 2014. Effect of diacylglycerol addition on crystallization properties of pure triacylglycerols. *Food Res. Int.* 55:436–444. <https://doi.org/10.1016/j.foodres.2013.11.037>.
- Smiddy, M. A., T. Huppertz, and S. M. van Ruth. 2012. Triacylglycerol and melting profiles of milk fat from several species. *Int. Dairy J.* 24:64–69. <https://doi.org/10.1016/j.idairyj.2011.07.001>.
- Szydłowska-Czernecka, A., G. Karlovits, M. Lach, and E. Szlyk. 2005. X-ray diffraction and differential scanning calorimetry studies of β' → β transitions in fat mixtures. *Food Chem.* 92:133–141. <https://doi.org/10.1016/j.foodchem.2004.07.010>.
- ten Grotenhuis, E., G. A. Van Aken, K. F. Van Malssen, and H. Schenk. 1999. Polymorphism of milk fat studied by differential scanning calorimetry and real-time X-ray powder diffraction. *J. Am. Oil Chem. Soc.* 76:1031–1039. <https://doi.org/10.1007/s11746-999-0201-5>.
- Tietz, R. A., and R. W. Hartel. 2000. Effects of minor lipids on crystallization of milk fat-cocoa butter blends and bloom formation in chocolate. *J. Am. Oil Chem. Soc.* 77:763–771. <https://doi.org/10.1007/s11746-000-0122-5>.
- Tzompa-Sosa, D. A., G. A. van Aken, A. C. M. van Hooijdonk, and H. J. F. van Valenberg. 2014. Influence of C16:0 and long-chain saturated fatty acids on normal variation of bovine milk fat triacylglycerol structure. *J. Dairy Sci.* 97:4542–4551. <https://doi.org/10.3168/jds.2014-7937>.
- van Aken, G. A., E. ten Grotenhuis, A. J. van Langevelde, and H. Schenk. 1999. Composition and crystallization of milk fat fractions. *J. Am. Oil Chem. Soc.* 76:1323–1331. <https://doi.org/10.1007/s11746-999-0146-8>.
- Van Aken, G. A., and K. A. Visser. 2000. Firmness and crystallization of milk fat in relation to processing conditions. *J. Dairy Sci.* 83:1919–1932. [https://doi.org/10.3168/jds.S0022-0302\(00\)75067-3](https://doi.org/10.3168/jds.S0022-0302(00)75067-3).
- Verma, A., N. S. Meitei, P. U. Gajbhiye, M. J. Raftery, and K. Ambatipudi. 2020. Comparative analysis of milk triglycerides profile between Jaffarabadi buffalo and Holstein Friesian cow. *Metabolites* 10:507. <https://doi.org/10.3390/metabo10120507>.
- Wang, F., Y. Liu, L. Shan, Q. Jin, X. Wang, and L. Li. 2010. Blooming in cocoa butter substitutes based compound chocolate: Investigations on composition, morphology, and melting behavior. *J. Am. Oil Chem. Soc.* 87:1137–1143. <https://doi.org/10.1007/s11746-010-1604-z>.
- Wang, X., H. Zhu, W. Zhang, Y. Zhang, P. Zhao, S. Zhang, X. Pang, J. Vervoort, J. Lu, and J. Lv. 2022. Triglyceride and fatty acid composition of ruminants milk, human milk, and infant formulae. *J. Food Compos. Anal.* 106:104327. <https://doi.org/10.1016/j.jfca.2021.104327>.
- Wang, Y., Y. Li, D. Yuan, Y. Li, K. Payne, and L. Zhang. 2019. Effect of fractionation and chemical characteristics on the crystallization behavior of milk fat. *J. Food Sci.* 84:3512–3521. <https://doi.org/10.1111/1750-3841.14961>.
- Zhao, P., S. Zhang, L. Liu, X. Pang, Y. Yang, J. Lu, and J. Lv. 2018. Differences in the triacylglycerol and fatty acid compositions of human colostrum and mature milk. *J. Agric. Food Chem.* 66:4571–4579. <https://doi.org/10.1021/acs.jafc.8b00868>.
- Zhu, H., A. Liang, X. Wang, W. Zhang, Y. Zhang, X. He, Y. Liu, S. Jiang, J. Lu, and J. Lv. 2021. Comparative analysis of triglycerides from different regions and mature lactation periods in Chinese Human Milk Project (CHMP) study. *Front. Nutr.* 8:798821. <https://doi.org/10.3389/fnut.2021.798821>.
- Zhu, H., X. Wang, W. Zhang, Y. Zhang, S. Zhang, X. Pang, J. Lu, and J. Lv. 2022. Dietary *Schizochytrium* microalgae affect the fatty acid profile of goat milk: Quantification of docosahexaenoic acid (DHA) and its distribution at Sn-2 position. *Foods* 11:2087. <https://doi.org/10.3390/foods11142087>.

ORCID

- Huiquan Zhu  <https://orcid.org/0000-0002-6771-8127>
Xiaoyang Pang  <https://orcid.org/0000-0003-1813-2039>
Shuwen Zhang  <https://orcid.org/0000-0002-0064-2236>
Jiaping Lv  <https://orcid.org/0000-0003-1526-7835>